EGSIEM
European Gravity Service for Improved Emergency Management

HORIZON 2020

EO-1-2014: New ideas for Earth-relevant space applications
Research and Innovation action

Action acronym:	**EGSIEM**
Action full title:	European Gravity Service for Improved Emergency Management
Grant agreement no:	637010

Deliverable D4.1
Concept of Scientific service

Date: 30/06/2016

Author(s): YJ, UM, FF

1.Change Record

Name	Author(s)	Date	Document ID
Draft 1	YJ, UM, FF	30/06/2016	D4.1
Draft 2			
Draft 3			

Table of Contents

2. Overview of Task 4.1

WP 4: Scientific Service, according to the EGSIEM proposal, aims at

- combination of the global monthly gravity models from the individual ACs,
- provision of user-friendly Level-3 products, and
- validation of the individual and the combined gravity field solutions.

It consists of work packages

- T4.1: Design and Concept,
- T4.2: Operation, and
- T4.3: External validation.

In T4.1 the required service products and data formats are defined. This includes Level-2 gravity field products (spherical harmonics) and Level-3 gravity field products (global grids in equivalent water heights).

Monthly gravity fields from the individual ACs are combined

- on solution level as a weighted average of the individual monthly solutions, or
- on normal equation level taking into account full correlations of the gravity field parameters with the pre-eliminated orbit- and satellite-specific parameters.

Relative weights are defined per gravity field solution and month. They are derived on solution level by variance component estimation (VCE). Normal equations are first scaled to contribute equally to a combined solution, in a second step the empirical weights derived on solution level are applied.

Considered for combination are all free (unbiased) individual contributions. To guarantee the quality (and unbiasedness) of the individual contributions and the combined solutions their signal content is evaluated in river basins, in Greenland and in selected regions of Antarctica. Outliers are detected by comparison to the arithmetic mean / median of all individual contributions.

The noise level of the individual and the combined solutions is studied on the level of anomalies (after subtraction of a deterministic model including bias, trend, annual and semi-annual variations) either as degree variances in the spectral domain or spatially by the standard deviation over regions with little short periodic variability (i.e., oceans).

3.Combination on Solution Level

3.1 General

Each EGSIEM AC contributes monthly gravity field solutions (and the corresponding normal equations) to the combination center at AIUB. Prior to the combination on normal equation level the individual solutions are compared and combined on solution level. This will enable

- quality monitoring of the individual solutions, and
- the derivation of empirical weights that are based on pairwise comparison of the individual solutions with their (weighted) mean.

The monthly gravity fields combined on solution level are expected to be more robust against outliers than the individual solutions. They are also expected to be less noisy due to the general reduction of white noise and approach specific colored noise. The empirical weights are re-used for the combination on normal equation level (see Sect. 4).

Quality control: The quality of the individual solutions is judged by studying their signal content within selected river and glacial basins and their noise level evaluating the short time variability over regions with little short periodic signal content, i.e., the oceans. The tools developed for quality monitoring of the individual ACs solutions are applied for quality control of the solutions combined on solution level as well as on normal equation level. Additional validation procedures using independent observation data will be developed in Task 4.3 (starting in M19).

Output and dissemination: All individual and the combined monthly solutions are provided as spherical harmonic coefficients (Level-2 Products) in the standard ICGEM-format (http://icgem.gfzpotsdam.de/ICGEM/documents_/ICGEM-Format-2011.pdf) used and maintained by the International Center for Global Earth Models (ICGEM), and are made available to the user community via the ICGEM and the Information System and Data Center 2.0 (ISDC2.0), currently under development at GFZ. Moreover global grids of equivalent water heights (Level-3 Products) will be computed (see Sect. 5) and distributed via the EGSIEM plotter (see Sect. 6 on Output and Dissemination).

Reports on the quality of the individual solutions and adopted weighting schemes will be distributed to the individual ACs and graphical representations will enable an easy monitoring of the performance of the individual ACs. This is fundamentally new in the gravity community and experience from the International GNSS Service (IGS) shows that this will lead to a competitive process driving innovation, as each AC will strive to improve the quality and increase the weight of the own results.

Test study: To test the tools for quality monitoring and to develop and test weighting schemes prior to the availability of monthly solutions from the individual EGSIEM ACs all time-series of monthly gravity field solutions publicly available at ICGEM were used. The derived combined solutions were provided to all EGSIEM and associated partners for validation and the weighting scheme reviewed based on the feedback of these test users.

3.2 Study of Combination on Solution Level

Since the NASA/DLR GRACE mission (Tapley et al. 2004) was launched in 2002, several different processing centers have produced GRACE gravity field solutions using GRACE GPS and K-band data. Considering only the geometrical orbit characteristics of the GRACE satellites (see Appendix 3.4.3), which orbit around the Earth approximately 15 times per day, monthly gravity fields could theoretically be computed up to a spherical harmonic resolution of about degree and order 200. But due to observation and processing noise monthly fields have to be truncated at much lower degrees (50, 60, 90, 96 or 120, depending on the processing center). Monthly GRACE gravity fields have been provided not only by the three official GRACE Science Data System (SDS) processing centers: CSR, GFZ, and JPL (Watkins et al. 2000), but also by additional processing centers outside the SDS, such as AIUB, ITSG, GRGS, TU Delft, and Tongji U. Each processing center adopts a different processing strategy to produce its GRACE gravity fields. The individual monthly GRACE gravity field solutions are available for public use at the ICGEM website[1]. For the purpose of a combination study this data base was used (Fig. 3.1).

Fig. 3.1: Combination of GRACE monthly gravity field solutions.

Prior to the combination, the tide system of all available individual solutions is standardized and they are scaled to common Earth parameters R_E and GM_E. Subsequently the different GRACE monthly gravity fields are investigated in terms of signal and noise in order to decide whether or not they are suitable for the combination. Regularized solutions that are discernable by attenuated signal amplitudes or unproportionally low and homogeneous noise levels have to be excluded to avoid signal attenuation in the combined solutions. The harmonized solutions are combined applying different weighting schemes and the combined solutions are validated in terms of signal and noise content and by comparison to external data. The flowchart of the combination on solution level is shown in Fig. 3.2. The final weighting scheme derived by this study eventually will be used for the EGSIEM combination on solution level (after the individual ACs contributions have become available).

[1] http://icgem.gfz-potsdam.de/ICGEM/

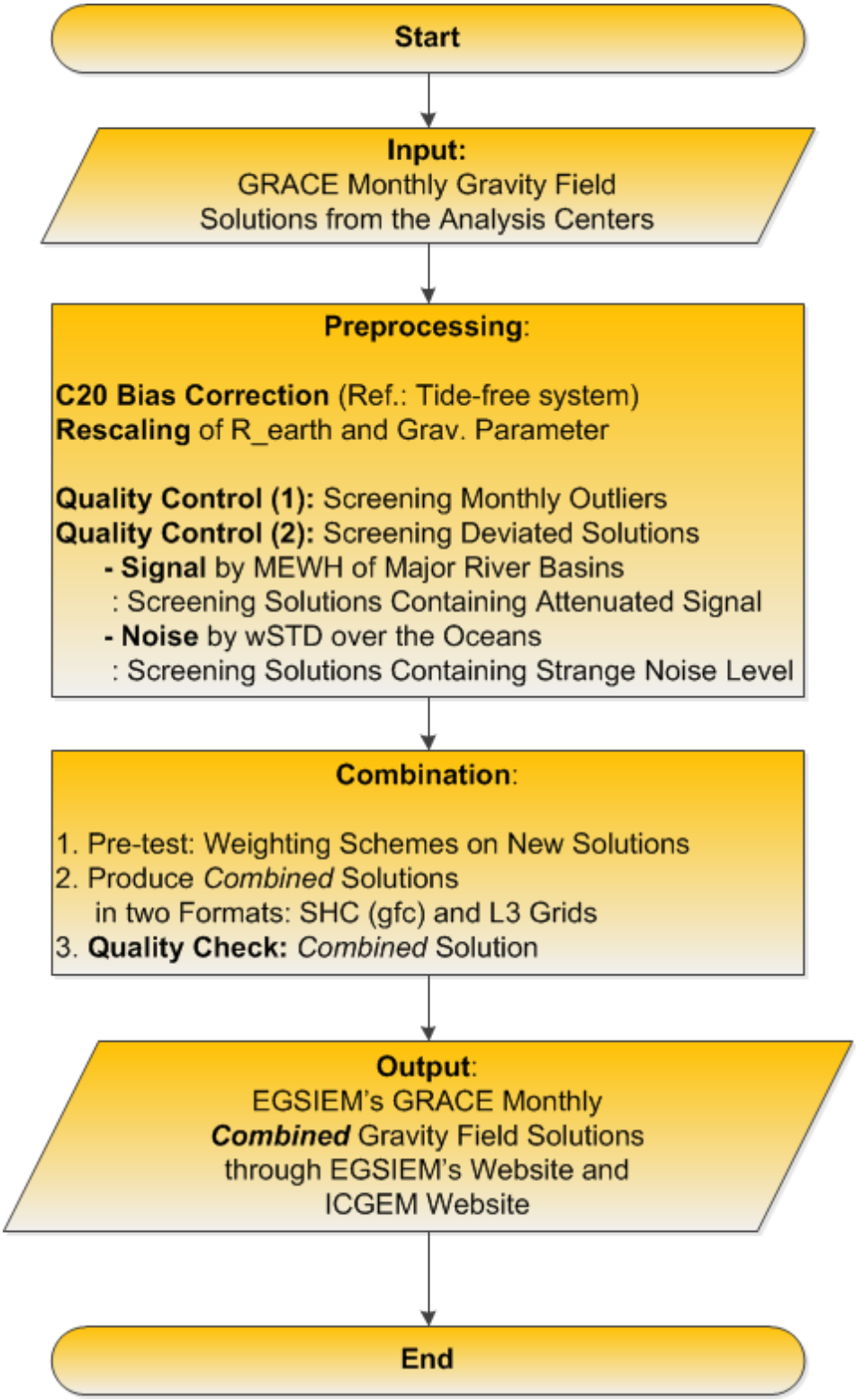

Fig. 3.2: Flowchart oft the combination on solution level

3.2.1 Input

The GRACE monthly gravity field solutions available officially at the ICGEM website as of May 2016 are shown in Tab. 3.1. Figure 3.3 shows the availability of the solutions over the GRACE mission period up to early in the year 2015. The data gaps in deep blue color in Fig. 3.3 appear frequently in early and late phases of the mission. They are related to poor data quality (in 2002) and phases of orbit resonance (in fall 2004, spring/summer 2012, and spring 2015). The periodic data gaps every 161 days starting in 2011 are due to battery problems of the GRACE satellites.

Tab. 3.1: Available time-series of GRACE monthly gravity field solutions

Analysis Centers	Release/Version	Maximum Degree	Processing Strategy	Reference
AIUB*	Release 2	60, 90	Celestial Mechanics Approach	Meyer et al. (2016)
GFZ*	Release 5a	90	Direct Approach	Dahle et al. (2012)
ITSG, TU Graz*	2014	60,90,120	Short arc approach (Empirical covariances)	Mayer-Gürr et al. (2014)
GRGS*	Release 3	80	Direct approach (regularized)	Bruinsma et al. (2010)
CSR	Release 5	60,90	Direct approach	Bettadpur (2012)
JPL	Release 5	60,90	Direct approach	Watkins and Yuan (2012)
TU Delft	Release 1	120	Acceleration approach (pre-filtered)	Liu et al. (2010)
Tongji U	Release 1	60	Short arc approach	Chen et al. (2015)

*: EGSIEM analysis center

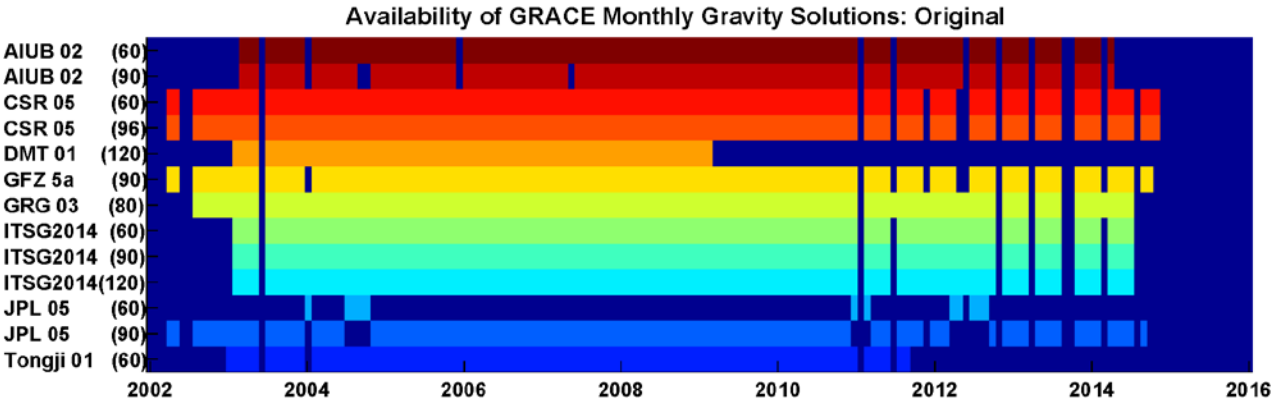

Fig. 3.3: Availability of GRACE monthly gravity field solutions throughout the GRACE mission period until 2015 (the deep blue color indicates that there is no solution available during that month.)

3.2.2 Preprocessing

Harmonization: The available GRACE monthly gravity field solutions (Tab. 3.1) have to be harmonized prior to combination. At first, the C_{20} coefficients of the individual monthly solutions are transformed to the same tide system (the tide-free system is chosen as a standard). Secondly, the monthly gravity field solutions referring to different Earth's radius R_E and Earth's gravitational parameter GM_E are rescaled to common values by using the equation (3.1) (Hofmann-Wellenhof and Moritz 2006):

$$\begin{Bmatrix} C_{lm} \\ S_{lm} \end{Bmatrix} = \left(\frac{GM_{sol}}{GM_{ref}}\right)\left(\frac{a_{sol}}{a_{ref}}\right)^{l} \begin{Bmatrix} C_{lm,sol} \\ S_{lm,sol} \end{Bmatrix} \qquad (3.1)$$

As reference values the ones are chosen which are most commonly used by the individual solutions: R_E=6378136.3m and GM_E=3.986004415×$10^{14}$$m^3$/$sec^2$ (both as recommended by the IUGG General Assembly 1991 in Vienna).

But even after harmonization the individual C_{20}-values agree poorly (Fig. 3.4) and therefore are ignored in the screening step and are excluded from further comparisons and when deriving relative weights. In Appendix 3.4.1, further comparisons of the C_{20} coefficients of different individual monthly gravity field solutions are given.

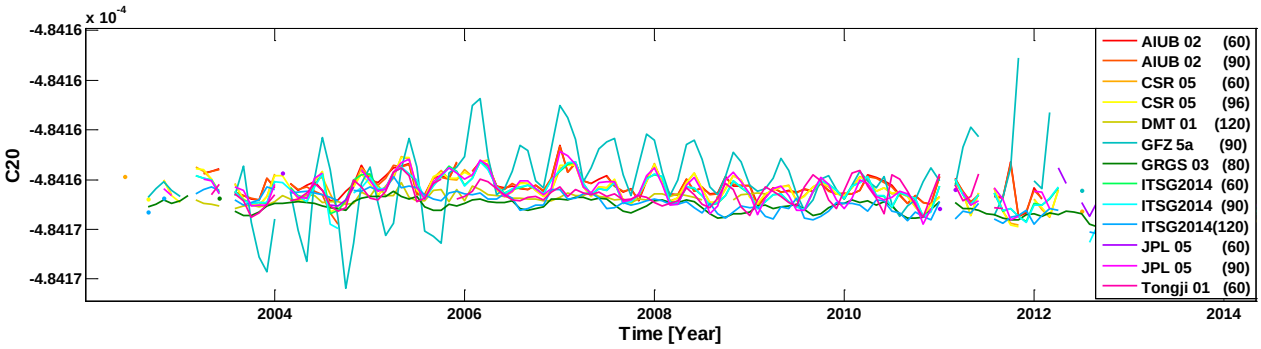

Fig. 2.4: Time series of the C_{20} coefficients of the individual monthly solutions.

Screening: After harmonization the monthly gravity field solutions are screened by using weighted standard deviations (wSTD) of the variability over the oceans as a quality measure to exclude outliers. wSTD are derived

- from monthly 1°-grids of equivalent water heights,
- after cell-wise subtraction of a deterministic model including bias, trend, annual and semi-annual variations to reduce the influence of slowly varying signal of oceanic origin,
- using only ocean grid cells after removal of a margin of 6° surrounding all coastlines to avoid signal leaking from the continents,
- weighting each grid cell by the cosine of the latitude (or sine of co-latitude) of its center point to account for the different cell sizes.

By relying on wSTD over the oceans as a measure of the noise we assume that the short time variability over the oceans is dominated by noise, which in our experience is a safe assumption. Using a threshold of three times the median absolute deviation (MAD, see Appendix 3.4.2) to exclude outliers, about 4.5% of the individual monthly gravity field solutions are screened out.

Grouping: For combination the monthly gravity field solutions are grouped by their maximum degrees: 60, 90, and 120. The individual solutions whose maximum degrees are not one of 60, 90, or 120 are cut to the nearest lower maximum degree. For example, the CSR's degree 96 solution is cut to degree 90 and the GRGS's degree 80 solution is cut to degree 60.

3.2.3 Comparison and Quality Control

The individual GRACE monthly gravity field solutions are compared in terms of signal and noise. If an individual solution has significantly attenuated signal or significantly more noise than other solutions, it may deteriorate the quality of the combined solution. For this reason a comparison of the individual monthly solutions has to be performed to sort out 'deviated' solutions before combination.

Signal: To compare the signal amplitudes in the individual solutions, the unitless spherical harmonic coefficients are transformed to equivalent water heights (EWH, see Wahr et al. (1998)) on a global grid. Mean equivalent water heights (MEWH) are computed by spatial averaging within hydrologically meaningful regions such as river basins. To account for their latitude-dependent size, grid-cells are weighted by the sine of the co-latitude θ of their midpoints:

$$MEWH = \frac{\sum EWH \cdot sin\theta}{\sum sin\theta} \qquad (3.2)$$

To reduce the noise the solutions may be filtered prior to the computation of MEWH. For filtering, a Gaussian-filter with a half maximum width of 300 km is applied. Fig. 3.4 shows MEWH of Amazon and Mekong river basins derived from the individual solutions.

Subsequently deterministic models containing bias, trend, annual and semi-annual variations are fitted to the MEWH of individual basins. The estimated annual variations and their formal errors are given for all individual solutions in the legend of Fig. 3.5. In Fig. 3.6 (top) the annual amplitudes for 12 of the major river basins (as listed in Tab. 3.2) and their formal errors are shown for a subset of the solutions (only degree 90). In Fig. 3.6 (bottom) additionally their basin-wise median and uncertainty ranges of three times the MAD (see Eqn. 3.2) are shown. Time-series of monthly gravity fields where the annual amplitudes do not agree within their formal errors with the majority of the other time-series in a significant number of basins, or that do not fit into the uncertainty range of three times MAD, are excluded from the combination. This is the case for the DMT time series that has reduced signal amplitude in 5 of the 12 basins. All other time-series agree well within their error bounds.

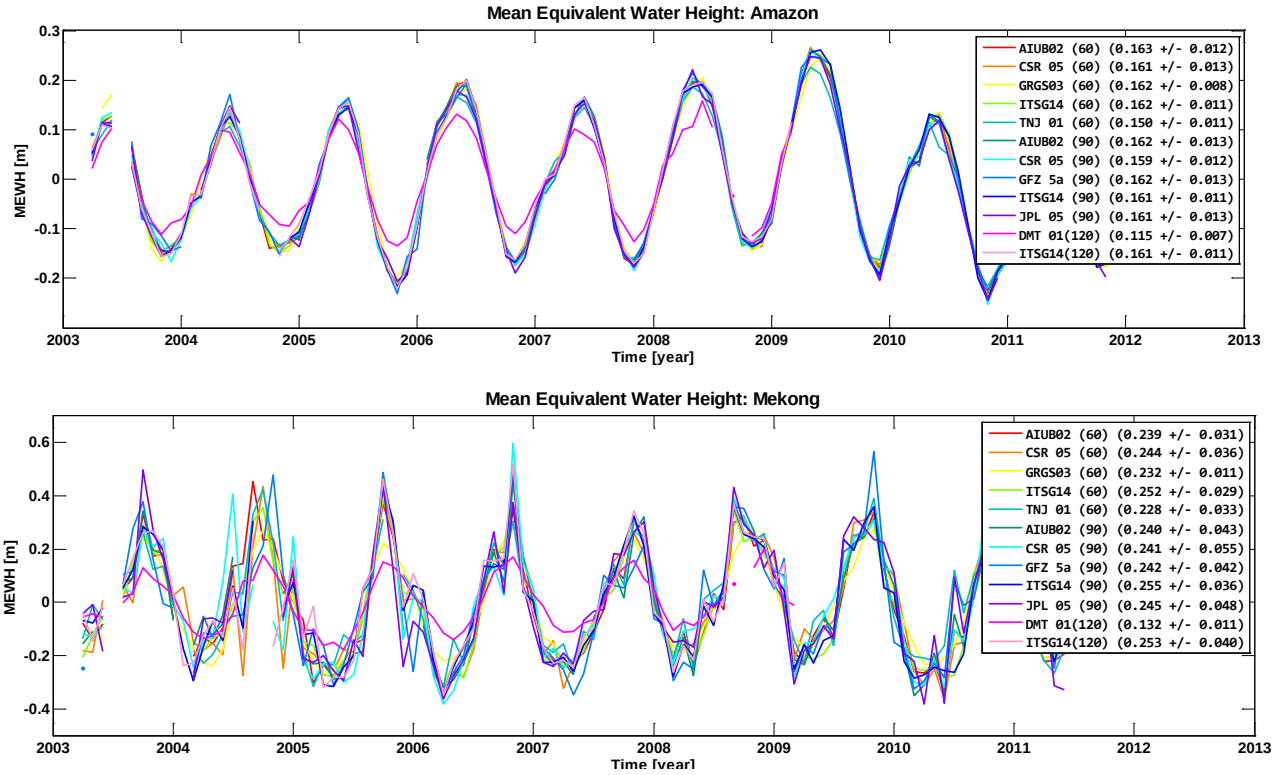

Fig. 3.5: MEWH of (top) Amazon and (bottom) Mekong river basins (the amplitude and formal error of estimated annual signal in each time series are given in the legend).

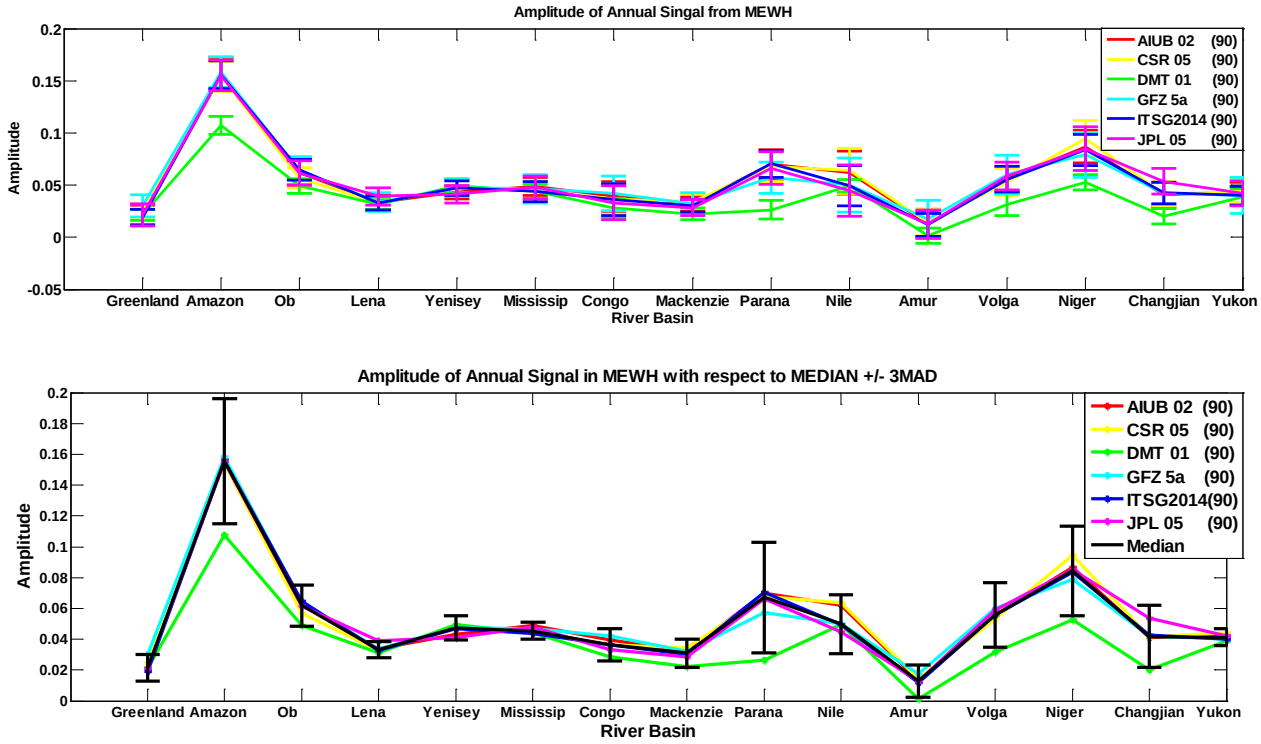

Fig. 3.6: MEWH amplitudes of the estimated annual variations in various major river basins, with two different criteria to examine possible attenuation of signals: (top) the error bars are the formal errors of the estimated amplitudes, (bottom) the median and uncertainty ranges of three times the MAD are included.

Tab. 3.2: Major river basins of which MEWHs are used as criterion to examine attenuation of signal.

	River Basin	*Continent*	*Size (km^2)*
1	Amazon	South America	6,144,727
2	Ob	Asia	2,972,497
3	Lena	Asia	2,306,772
4	Yenisey	Asia	2,554,482
5	Mississippi	North America	3,202,230
6	Congo	Africa	3,730,474
7	Nile	Africa	3,254,555
8	Prana	South America	2,582,672
9	Mackenzie	North America	1,743,058
10	Amur	Asia	1,929,981
11	Volga	Europe	1,410,994
12	Niger	Africa	2,261,763
13	Yangtze (Chang Jiang)	Asia	1,722,155
14	Yukon	North America	847,642

Noise: The individual solutions are compared in terms of noise using the wSTD over the oceans (see Sect. 3.2.2). Figure 3.7 shows the wSTD over the oceans derived from the raw and smoothed degree 60 and 90 individual solutions. The median of wSTD per time series is given in the legend. Most of the individual solutions show comparable levels of noise. However, the GRGS solution shows significantly lower noise than other individual solutions due to regularization.

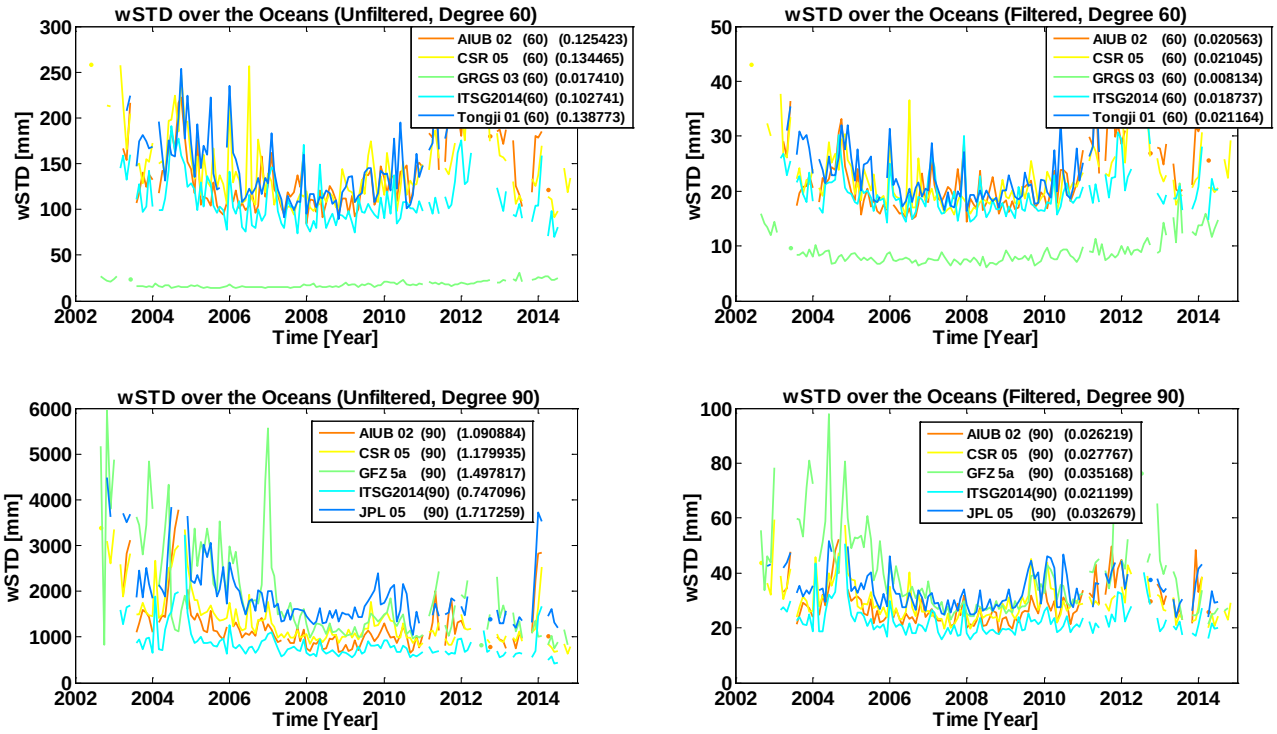

Fig. 3.7: wSTD over the oceans using the degree 60 (top) and 90 (bottom) individual solutions without (left) and with (right) filtering (the median of wSTD per time-series is given in the legend).

To further assess the noise of the individual solutions the formal errors are studied. GRGS shows a very different pattern of coefficient wise formal errors as compared to the other solutions (Fig. 3.8). The formal errors of the other individual solutions increase with increasing degree and order. However, the GRGS solution as well as the DMT solution show reversed patterns especially in high-degree and high-order coefficients due to their regularization. Because the danger of signal attenuation is closely connected to any regularization, the GRGS solution is also not included in the combination.

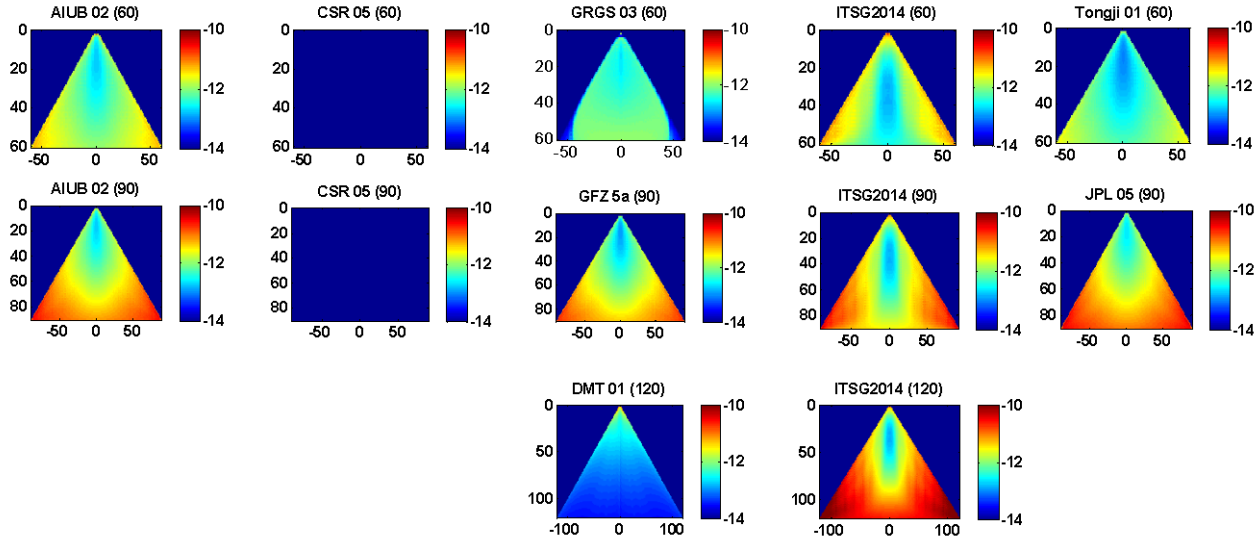

Fig. 3.8: Formal errors of the C and S coefficients of the individual monthly solutions in August 2008 (note that for CSR no formal errors are provided).

3.2.4 Relative weighting

The individual solutions can be combined without adopting any weights. This corresponds to the arithmetic mean of the individual solutions. However, the individual solutions have different noise levels as shown in Fig. 3.7. Hence, a weighted combination may be expected to provide a better solution than the simple arithmetic mean. As a first approach to find the best weighting scheme among the possible weighting methods, weights based on the components of variance are examined. Basically, the weights are derived by the inverse of the square of the difference from the arithmetic mean. Table 3 shows the different weighting schemes that were tested in this study.

Tab. 3.3: Weighting schemes for combination of GRACE monthly solutions.

Weight	Applied	Formula
Coefficient-wise weight	Per Order, Degree, Month	$w_{l,m}^{i,t} = \left[\left(X_{l,m}^{i,t} - \bar{X}_{l,m}^{t}\right)^2\right]^{-1}$
Order-wise weight	Per Order, Month	$w_{m}^{i,t} = \left[\frac{1}{l_{max} - m + 1}\sum_{l=m}^{l_{max}}\left(X_{l,m}^{i,t} - \bar{X}_{l,m}^{t}\right)^2\right]^{-1}$
Single weight	Per Month	$w^{i,t} = \left[\frac{1}{N_{Coeff}}\sum_{c=1}^{N_{Coeff}}\left(X_{l,m}^{i,t} - \bar{X}_{l,m}^{t}\right)^2\right]^{-1}$
VCE	Per Month	$w_{iIter}^{i,t} = \left(1 - \frac{w_{iIter-1}^{i,t}}{\sum_{iSol=1}^{nSol} w_{iIter-1}^{i,t}}\right) \cdot \frac{1}{RMS(X_{l,m}^{i,t} - \hat{X}_{l,m}^{i,t})}$

i: individual solution, t: time [month], l: degree, m: order, l_{max}: maximum degree, $iIter$: iteration number
N_{Coeff} : number of spherical harmonic coefficients in a solution, N_{Sol} : number of solutions involved in combination,
X_{lm}: spherical harmonic coefficient $\left[{C_{lm}}^T \quad {S_{lm}}^T\right]^T$, $\bar{X}_{l,m}^{t}$: average of coefficients $X_{l,m}^{i,t}$ from all involved solutions
$\hat{X}_{l,m}^{t}$: weighted average of coefficients $X_{l,m}^{i,t}$ from all involved solutions

Coefficient-wise weighting: The coefficient-wise weights are derived for each individual coefficient using the formula shown in Table 3. Figure 3.9 shows the average of the coefficient-wise weights of the individual degree 60 and 90 solutions over the whole time span (2003 to 2011 for degree 60, 2003 to 2014 for degree 90). In the degree 60 case, the AIUB, CSR, and ITSG solutions have slightly larger weights than the Tongji U solution. In the degree 90 case, the AIUB, CSR, and ITSG solutions have relatively larger weights than the GFZ and JPL solutions. The AIUB solution's resonance-order coefficients, the CSR solution's low-degree and low-order coefficients, the GFZ solution's resonance-order coefficients, the ITSG solution's degree 3 and zonal coefficients, and JPL solution's high-degree and low-order coefficients have relatively lower weights. Low weight indicates that the coefficient of an individual gravity field shows a larger deviation from the arithmetic mean than the coefficients of the other contributing solutions.

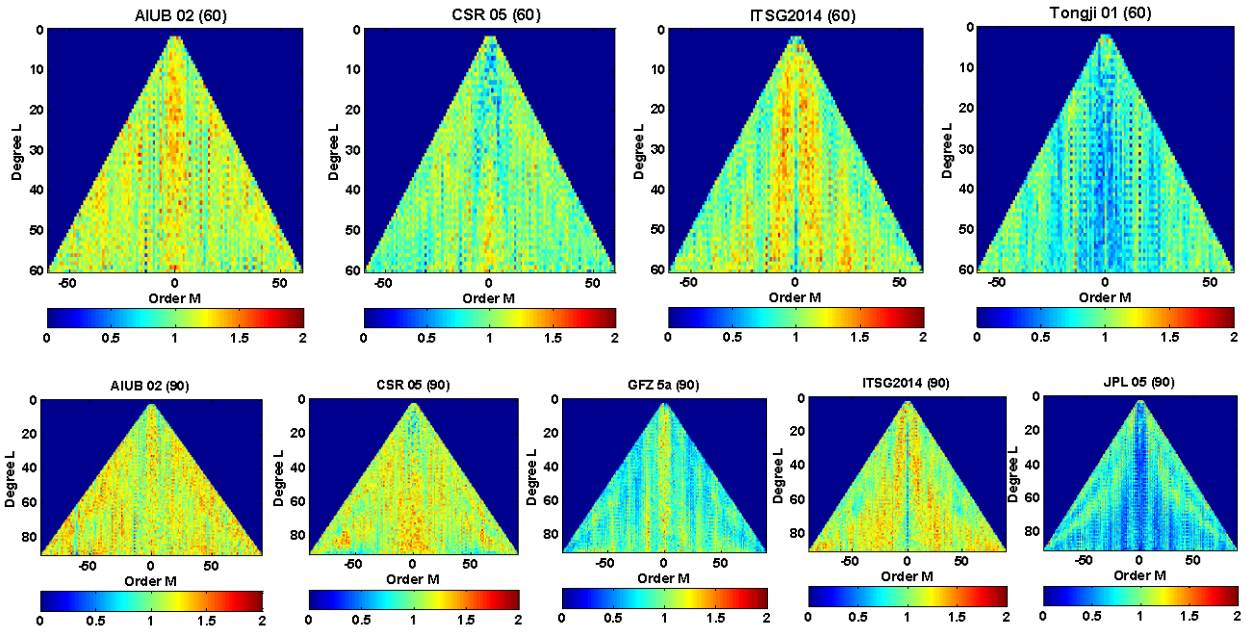

Fig. 3.9: Average of coefficient-wise weights on the (top) degree 60 and (bottom) degree 90 solutions.

The zonal coefficients of the ITSG solutions are obviously systematically different from other time series. Examination of the star camera + accelerometer sensor fusion data solely used by ITSG revealed a systematic effect on the zonal coefficients that is most probably the reason for this difference. More about the tests concerning the sensor fusion data can be found in Appendix 3.4.4.

Order-wise weighting: In Fig. 3.9, the weights of the individual coefficients show order-specific features. The coefficient-wise weights can be condensed into order-wise weights (see formula in Tab. 3.3). Figure 10 shows these order-wise weights for all individual solutions. The weights of the low-order coefficients of the degree 60 Tongji solution decrease since the year 2008. The order-wise weights on the GFZ solution reflect the time dependent noise level as revealed by the wSTD over the oceans (see Fig. 3.7). Figure 3.11 shows order-wise weights averaged over the whole time spans. The AIUB, CSR, and ITSG solutions generally show higher weights than the other solutions in both degree 60 and 90 cases. However, the order-wise weights of the resonance-orders such as 16, 31, 46, and 61 are similar to one another for all of the individual solutions because the coefficients of resonance orders are of an inferior quality for all solutions.

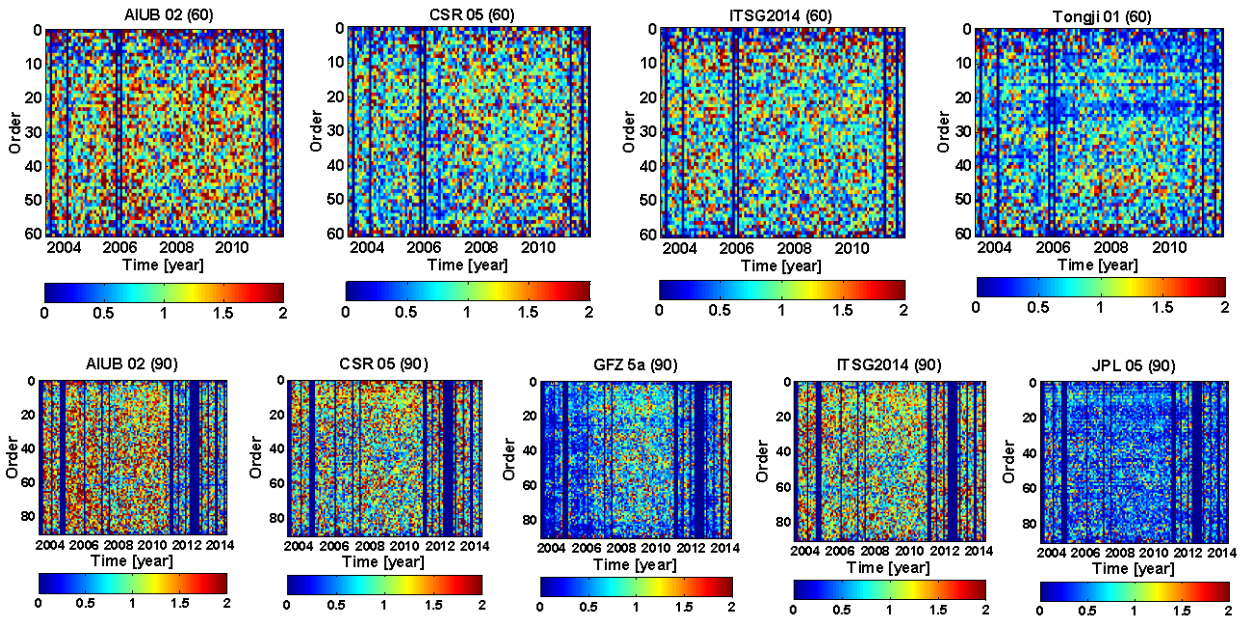

Fig. 3.10: Order-wise weights in case of (top) degree 60 or (bottom) degree 90 solutions.

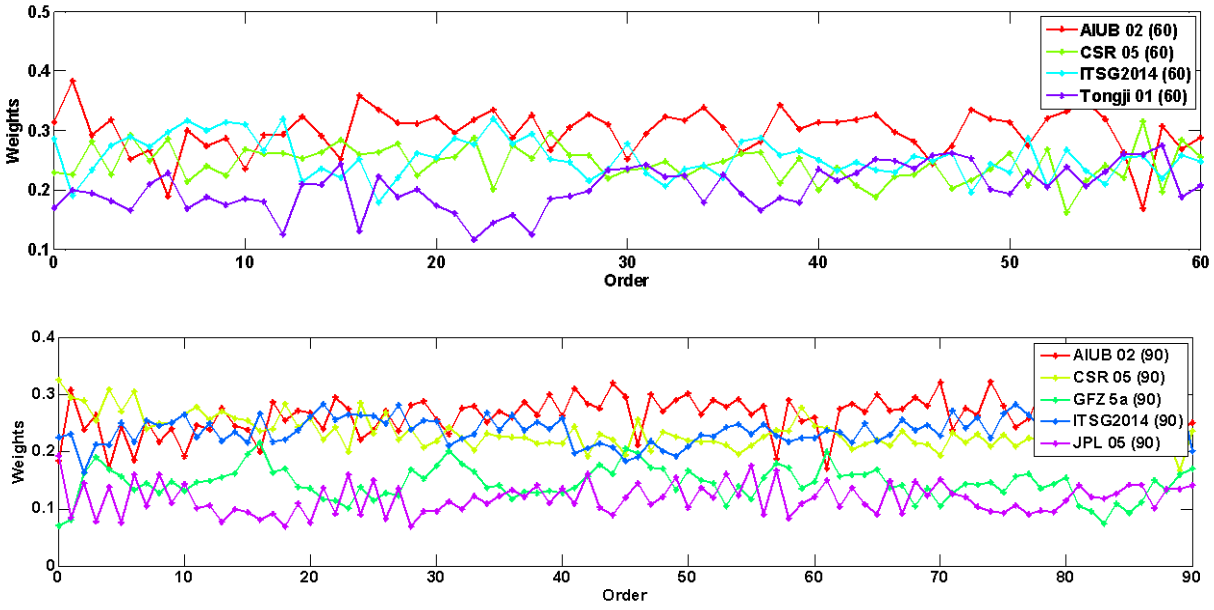

Fig. 3.11: Order-wise weights averaged over the whole time span of (top) degree 60 or (bottom) degree 90 solutions.

Single weight per solution: The coefficient-wise and order-wise weights show that the relative level of weight of each individual solution is more or less constant over most of the coefficients or orders. Based on this finding, one single weight per month and gravity field may be enough to characterize the individual solutions. Such a weighting scheme is also preferred due to its simplicity. Figure 3.12 shows the single weight for each solution as a function of time. The overall relative levels of weights are very similar to those of the order-wise weights. The temporal evolution of the weights of the GFZ solution reflects the increased noise level of this solution early and late during the mission (see Fig. 3.7).

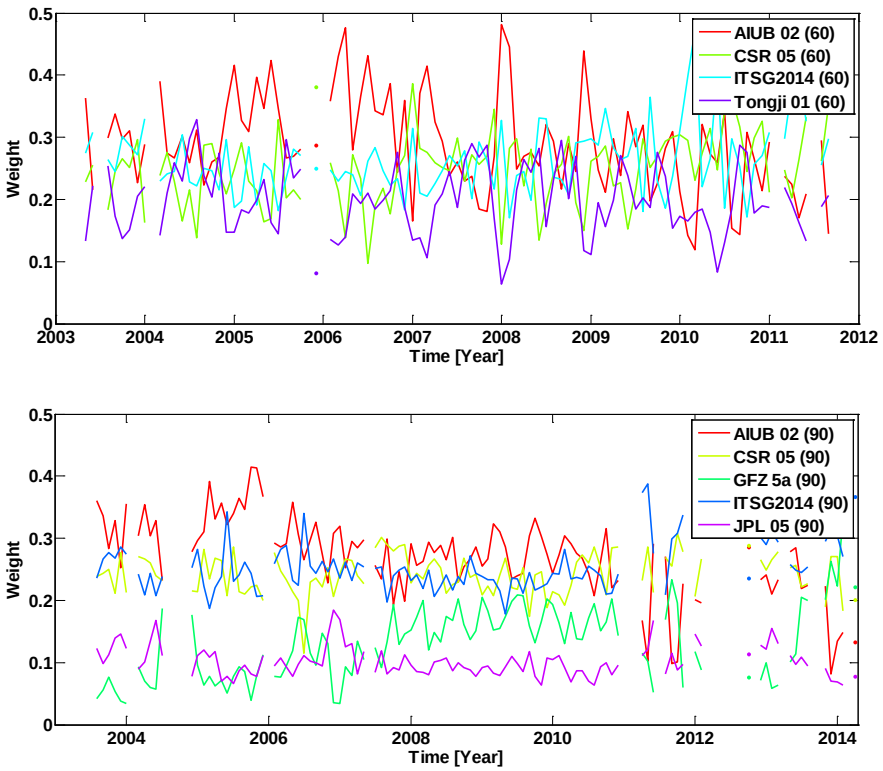

Fig. 3.12: Single weight per month of (top) degree 60 or (bottom) degree 90 solutions.

Weights derived iteratively using Variance Component Estimation: The experiments so far revealed different noise levels in the individual solutions. In extreme cases weights derived by comparison to the arithmetic mean may not be enough to take the different noise levels into account, because the arithmetic mean is impaired by the noise. This problem is commonly solved deriving the weights iteratively by Variance Component Estimation (VCE). VCE is basically an iterative process where the mean as well as the weights derived from pairwise comparison to this mean are updated in each iteration step (see formula in Tab. 3.3). Fig. 3.13 shows two examples of weights derived iteratively using the VCE method. The weights are usually converged after the third or fourth iteration.

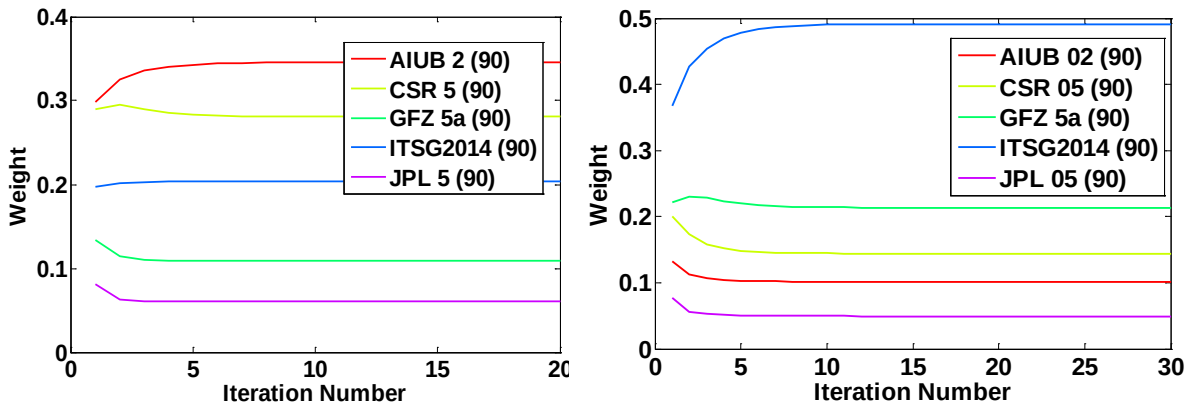

Fig. 3.13: Weights derived iteratively using VCE for (left) 2007/08 and (right) 2014/03.

3.2.5 Weighted Combination

Using the weights derived in Sect. 3.2.4, combined solutions are generated according to:

$$\hat{X} = \frac{\sum_{iSol=1}^{nSol} w_{iSol} X_{iSol}}{\sum_{iSol=1}^{nSol} w_{iSol}} \qquad (3.3)$$

where w_{iSol} is the weight of the individual solution iSol and X_{iSol} stands for the spherical harmonic coefficients of solution iSol. The combination procedure is discussed and first test combinations are presented in Jean et al. (2015a, 2015b), Bruinsma et al. (2015) and Jäggi et al. (2015).

Fig. 3.14 shows the MEWH of Greenland derived from the individual solutions and from the weighted combination using single weights per month and solution (derived without iteration by VCE). In the unfiltered case (left) the combined solutions show less scatter than most of the individual solutions, while the size of the negative trend (see legend) is maintained.

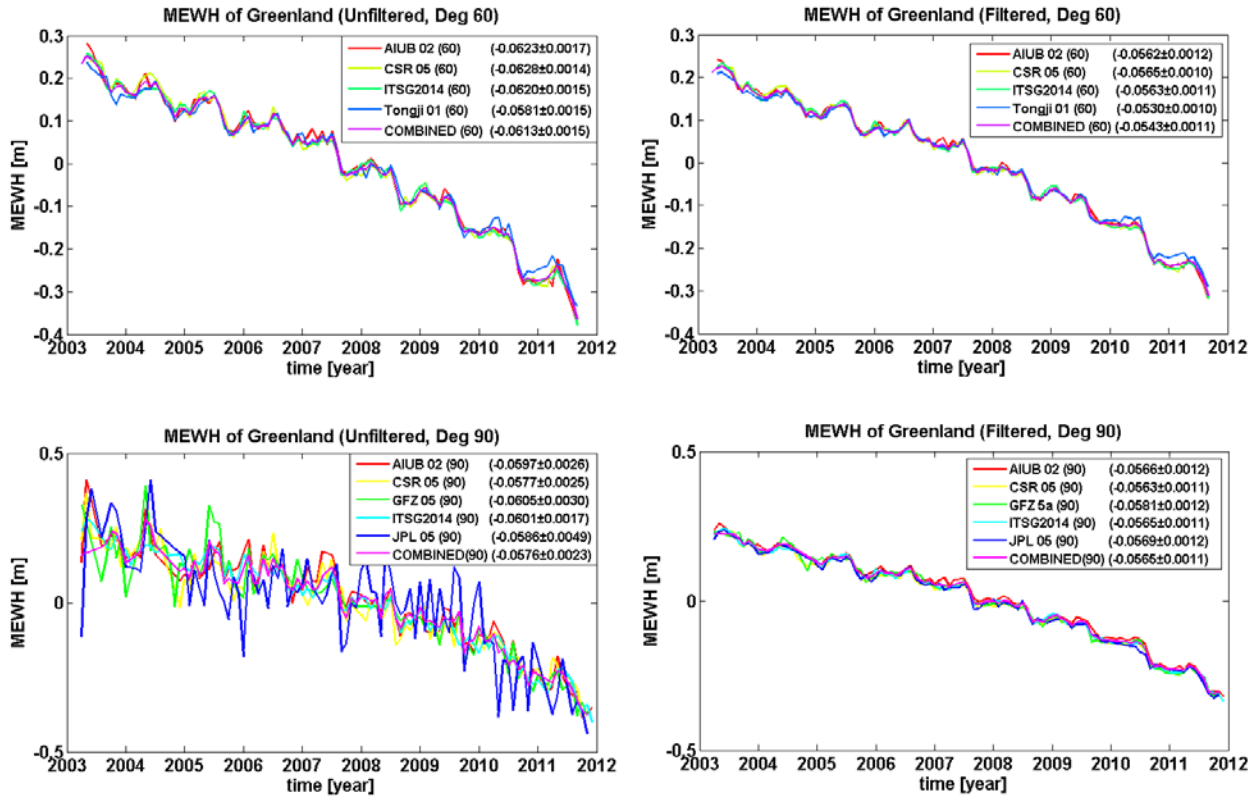

Fig. 3.14: MEWH of Greenland derived from the individual solutions and from the weighted combination, (top) degree 60, (bottom) degree 90, (left) unfiltered, (right) smoothed. Estimated trends and their formal errors are provided in the legend.

Figure 3.15 shows the wSTD over the oceans of the individual solutions and the combined solutions using the four different weighting schemes: arithmetic mean, coefficient-wise weighting, order-wise weighting, and single-weight. The degree 60 combinations (top) show significantly reduced noise in both, the unfiltered (left) and the smoothed (right) case. However, in case of the degree 90 combinations, one individual solution (ITSG-2014) during certain months is less noisy than the combined solutions.

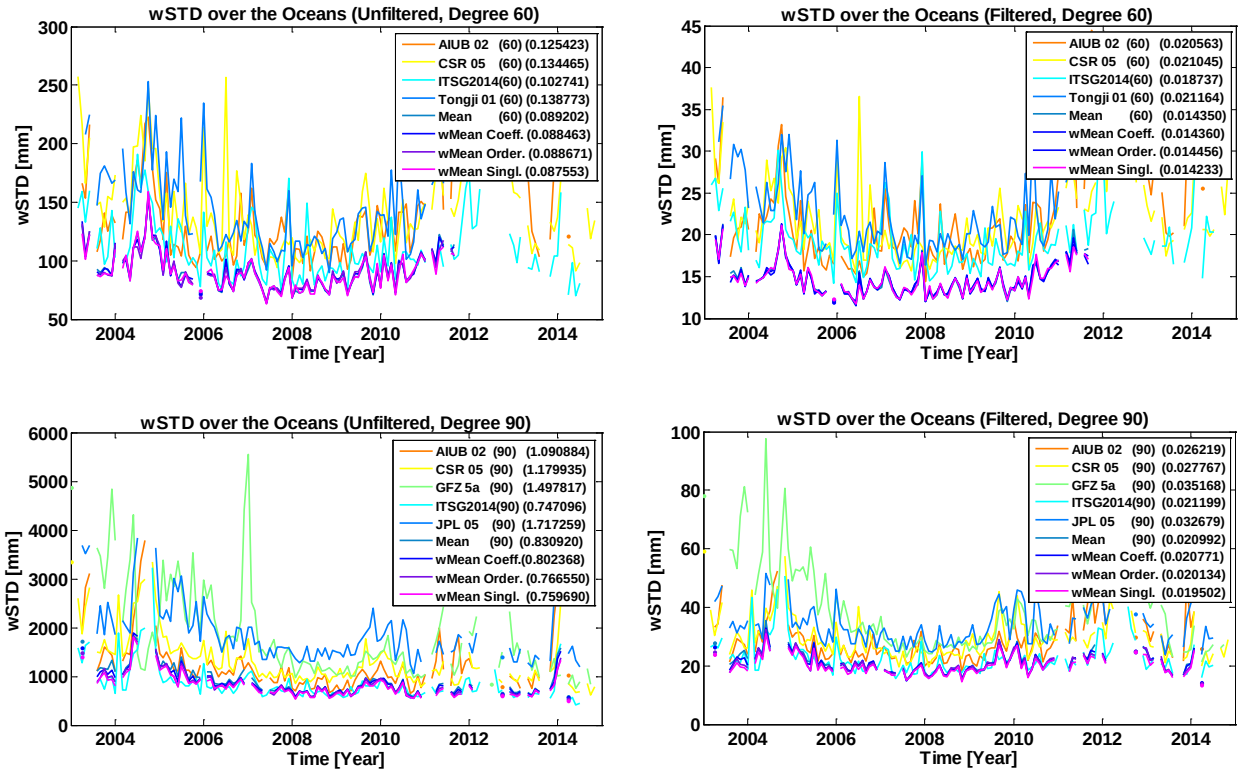

Fig. 3.15: wSTD over the oceans of the individual and the combined solutions, (top) degree 60, (bottom) degree 90, (left) unfiltered, (right) smoothed.

Fig. 3.16 shows the median of the time series of degree variances of anomalies that were computed by coefficient-wise fit and subtraction of the deterministically modeled major time variations (including bias, trend, annual and semi-annual variations). The degree variances were computed from orders up to 29 only, because beyond degree 29 the modeled time variations are governed by colored noise in the coefficients and anomalies cannot be defined meaningfully. The degree 60 combinations have less noise than all individual solutions, while in case of the degree 90 combinations, the one individual solution with the lowest noise level has smaller degree variances beyond about degree 60. This validation indicates that the combined solutions have the least noise up to degree 60, but are not necessarily throughout the whole spherical harmonic spectrum.

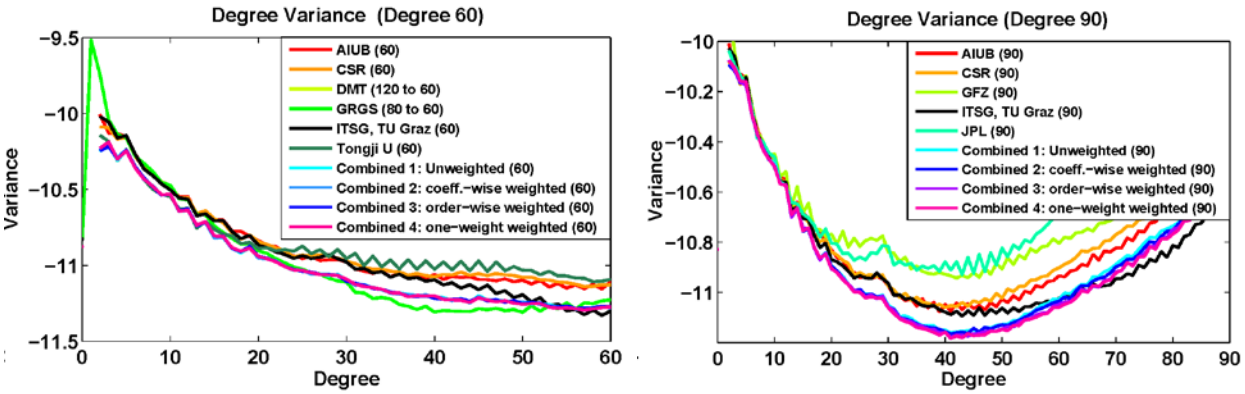

Fig. 3.16: Median of degree variances of time series of anomalies, (left) degree 60, (right) degree 90.

There are several possible reasons of this phenomenon:

- The noise levels of the individual solutions may be so different that the derivation of weights has to be iterated by VCE (meanwhile it was shown that VCE does not lead to significantly different results).
- The anomalies may not be representative for the actual noise level of the coefficients; this surely is the case since the anomalies count both noise and non periodic signal as noise. But this is an unlikely reason for the observed phenomenon because especially at high degrees the anomalies should be dominated by noise.
- One individual solution shows attenuated signal that is punished by low weights, i.e., low contribution to the weighted combination, but rewarded by the anomalies that are generally smaller in case of attenuated variability. This case should be excluded by the careful assessment of the individual solutions prior to combination.
- One individual solution is systematically different (better) from the majority of solutions contributing to the combination and at the same time less noisy. In this case the arithmetic mean does not represent the truth and the individual solution is punished by low weights. Nevertheless it shows small anomalies due to its low noise level.

To further investigate these cases a simulation study was performed (Sect. 3.2.6). Here it is anticipated that the last reason was identified to be the probable cause for the failure of the combination to show the smallest variability throughout the whole spherical harmonic spectrum. It has to be stressed that this simulation study was performed with the time-series available at ICGEM and not the improved EGSIEM solutions (to be derived in WP2). So the observed phenomenon may become a non-issue. If not, then all of the EGSIEM ACs are invited to further improve their individual solutions to finally contribute to a combined solutions that is superior to the individual solutions at all degrees.

3.2.6 Simulation study

As shown in Figs. 3.15 and 3.16, the combined solutions are only superior to the best individual contribution for part of the spherical harmonic spectrum. Basically, the combined solutions have less noise than the individual ITSG solution up to degree 60. At higher degrees the ITSG solution has smaller anomalies, i.e., less non-seasonal variability than the combined solution. To investigate possible reasons for this behavior, a simulation study is designed and performed.

As mentioned above, a possible reason for the observed phenomenon may be systematic differences between the ITSG solution and all other individual solutions. To investigate the effect of systematic (colored) noise in the presence of white noise of different levels, four different simulation cases are designed. At first, a reference solution is generated. For this purpose bias $a_{0,lm}$, trend $a_{1,lm}$ and periodic annual variations with sine and cosine amplitudes $a_{2,lm}$ and $b_{2,lm}$, respectively, are fitted to the time series of coefficients of the combined solution (derived in Sect. 3.2.5 using single weights per month) and this deterministic model, evaluated at a certain epoch, is defined to represent the true signal.

$$\hat{X}_{lm}(t) = a_{0,lm} + a_{1,lm}\Delta t + a_{2,lm} \sin \omega \Delta t + b_{2,lm} \cos \omega \Delta t \qquad (3.4)$$

The simulated solutions are generated by adding a white noise term ϵ with an RMS of 1 to the reference solution and multiplying a scale factor k_i to each term (including the random noise term ϵ):

$$\boldsymbol{X_{i_{lm}}(t) = k_0 a_{0_{lm}} + k_1 a_{1_{lm}} \Delta t + k_2 (a_{2_{lm}} \sin \omega \Delta t + b_{2_{lm}} \cos \omega \Delta t) + k_3 \epsilon} \qquad (3.5)$$

The scale factors applied to the model of the true signal are shown in Tab. 3.4. For the sake of simplicity only the amplitude of the periodic annual signal and the white noise are varied by the scale factors, the first to simulate systematic signal attenuation that may be caused by regularization, the latter to account for different levels of white noise.

Tab. 3.4: Coefficients of model and scale factors applied to the model

Coefficient	Term	Scale Factor	In the simulation
a_0	Bias	k_0	Fixed
a_1	Trend	k_1	Fixed
a_2, b_2	Annual Signal	k_2	Varied
ϵ	Random Error	k_3	Varied

Figs. 3.17 and 3.18 show the cases investigated in this simulation study. The cases 1 to 3 are designed to investigate the effect of different levels of white noise on the combination. In case 4 the effect of systematic errors, i.e., attenuated signal amplitude, in the presence of white noise is investigated. In each case, four simulated individual solutions and their combination are generated and compared in terms of signal and noise.

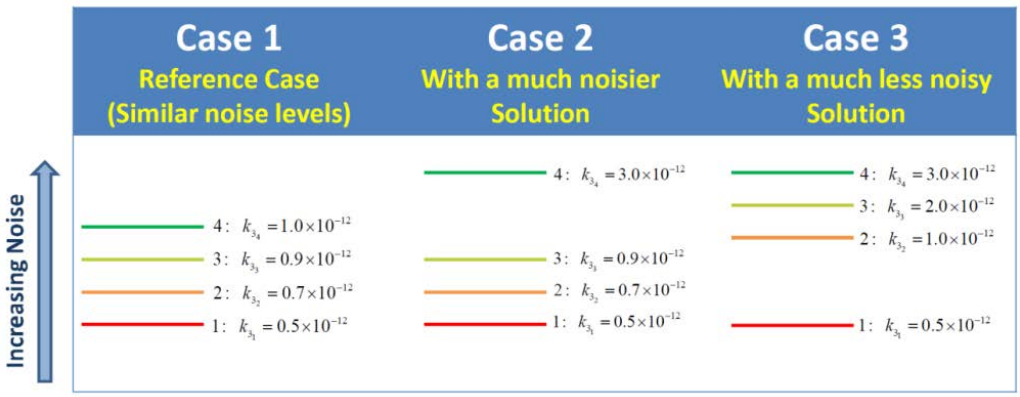

Fig. 3.17: Simulation cases with different levels of white noise.

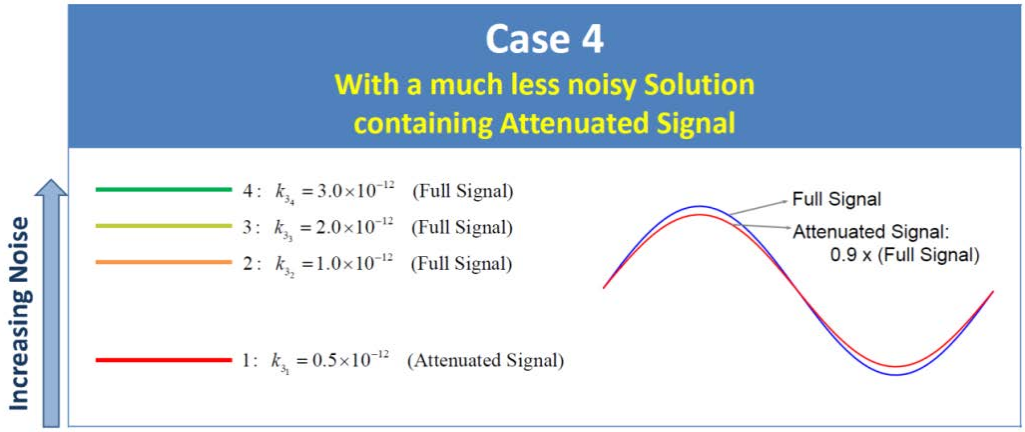

Fig. 3.18: Simulation case including an individual solution with systematic errors (signal attenuation to 90% of full signal) in combination with a low level of white noise.

Simulation case 1 is designed to show a reference case where the simulated individual solutions are closely related without any outliers in terms of noise. As shown in Fig. 3.19 (top), the combined solutions (iterated by VCE) in this case have significantly less noise than any of the individual solutions in both wSTD over the oceans (left) and the median of degree variances of anomalies (right).

Case 2 resembles a situation where one individual solution has an extremely high level of white noise compared to all other individual solutions. In this case, only the noise levels of the weighted combined solutions are better than the individual solutions while an arithmetic mean is not superior to all individual solutions (Fig. 3.19, middle row). The weighted combination can be slightly improved by iteration (VCE).

In case 3 a solution with an extraordinary low level of white noise is included. Again the arithmetic mean does not lead to a combination better than all individual solutions and even the weighted combination without iteration is still worse than the best individual solution (Fig. 3.19, bottom). Only after iteration the combined solution is superior to all individual solutions. So in this case it is indispensable to use variance component estimation.

The case 4 is different from the previous three cases. The noise levels of the simulated individual solutions in this case are the same as those in the case 3. However, in this case the signal content of the individual solution containing the lowest noise is reduced by 10%. This kind of effect can easily be produced by regularization and therefore has to be rated as a rather realistic scenario. Now the amplitude of the combined solutions is slightly reduced and only recovers after iteration (Fig. 3.20, left). The median of the degree variances of the anomalies (Fig. 3.20, right) exhibits a behavior that resembles the case encountered in Sect. 3.2.5 when combining the real monthly gravity field solutions of different processing centers. After iteration the noise level of the combined solution converges on the noise level of the second best solution (in terms of white noise). Obviously the weights of the individual solution with attenuated signal are dominated by the systematic difference in signal content and not by the different levels of white noise.

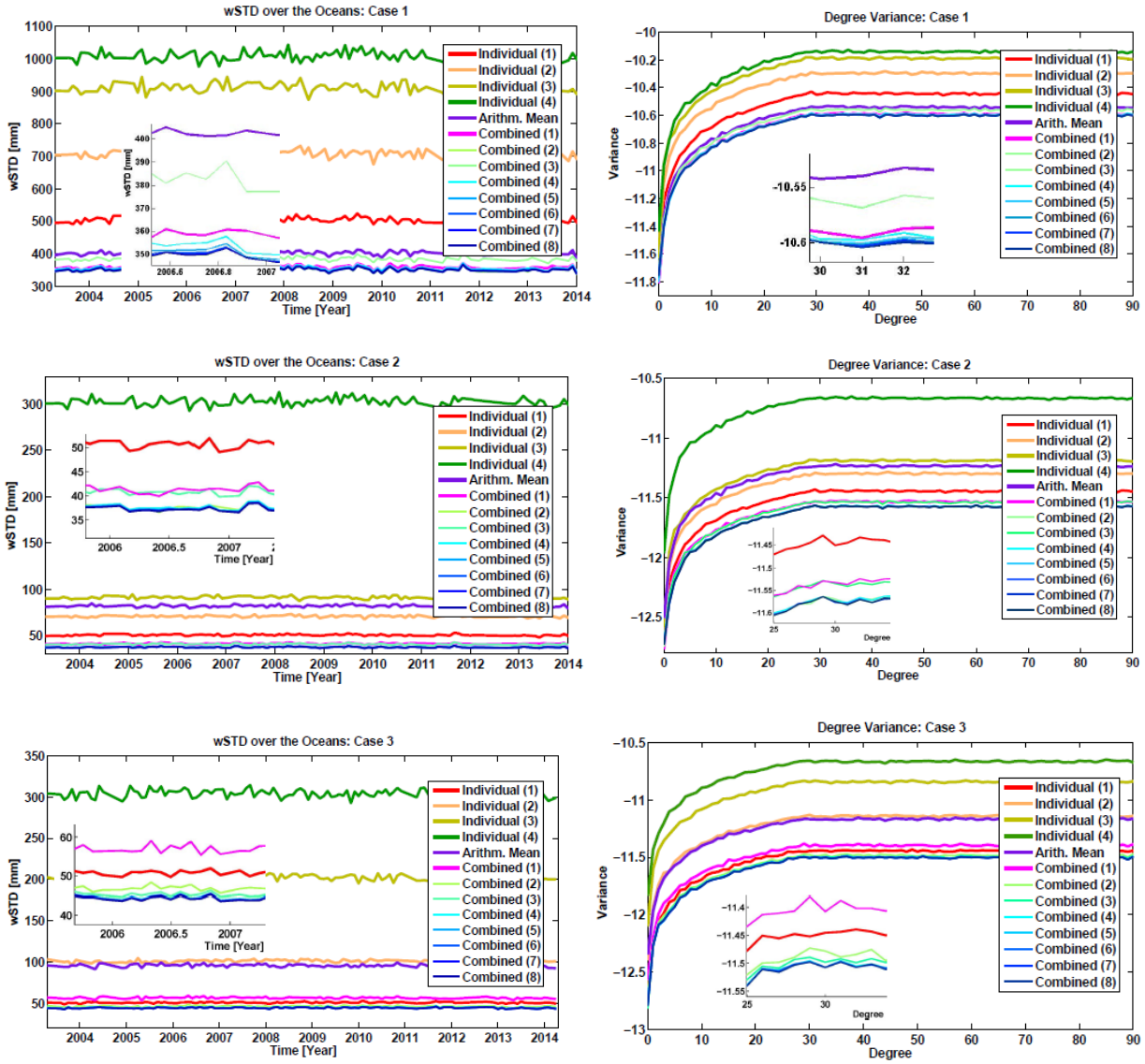

Fig. 3.19: wSTD over the oceans (left) and median of degree variances of anomalies (right) of the individual solutions of simulation cases 1 to 3 and their combinations (the numbers after 'Combined' in the legends indicate the number of iterations). The inlays show zooms into part of the figures to better visualize the effect of the iteration.

The results of the simulation imply that the results achieved by the combination of real gravity fields may be caused by signal attenuation in the individual ITSG time series. But this possible signal attenuation could not be identified by the quality check in Sect. 3.2.3. So we have to consider the possibility that any other systematic difference between one individual solution and the majority of solutions may also cause comparable effects. Since ITSG is the only processing center applying empirical covariances as a noise model it is well possible that systematic differences exist. From the quality checks performed in the frame of the EGSIEM combination service it is not possible to judge whether the ITSG solutions or the majority of other solutions are better (in terms of signal content; the noise level of the ITSG solutions obviously is very low). So here we rely on the external validation that will be performed in task 4.3.

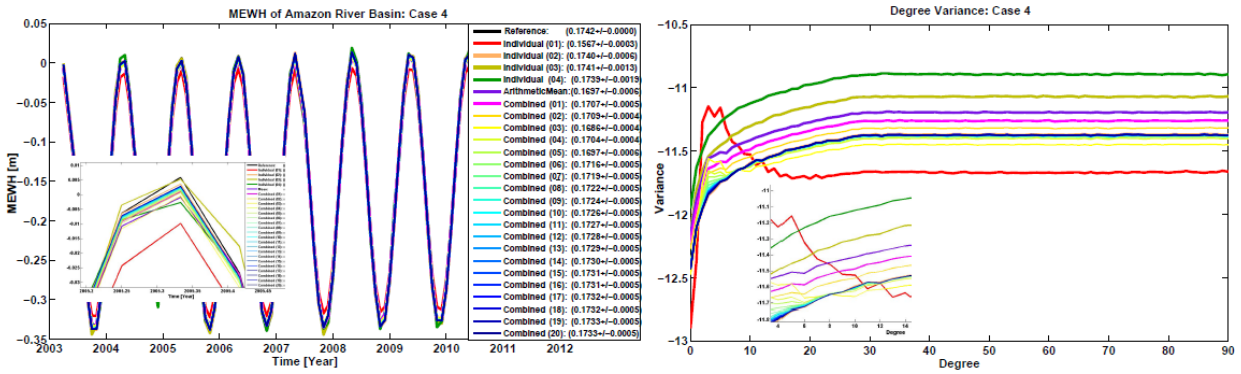

Fig. 3.20: MEWH of the Amazon river basin (left) and median of degree variances of anomalies (right) of the simulated individual solutions and their combinations in case 4. The amplitudes of the estimated annual signals are given in the legend. The inlays show zooms into parts of the figures to visualize the effect of the iteration.

The results of the simulation study also suggest that iteration by VCE may cure the problem of attenuated signal in an individual solution. Therefore we include the DMT solution in the combination that was excluded by the quality check (Sect. 3.2.3). In Fig. 3.21 the MEWH of the Amazon river basin are shown. The attenuated signal in the DMT solution clearly has a negative impact on the combined solution. The full signal amplitude cannot be recovered, even after iteration. So we have to conclude that in this case the weights of the individual solutions are dominated by the extremely different levels of white noise and not by the systematic effect of signal attenuation in the DMT solutions. To exclude this case we have to execute the quality check as described in Sect. 3.2.3 and cannot just rely on VCE to cure the problem. The results of the simulation study are further discussed in Jean et al. (2016).

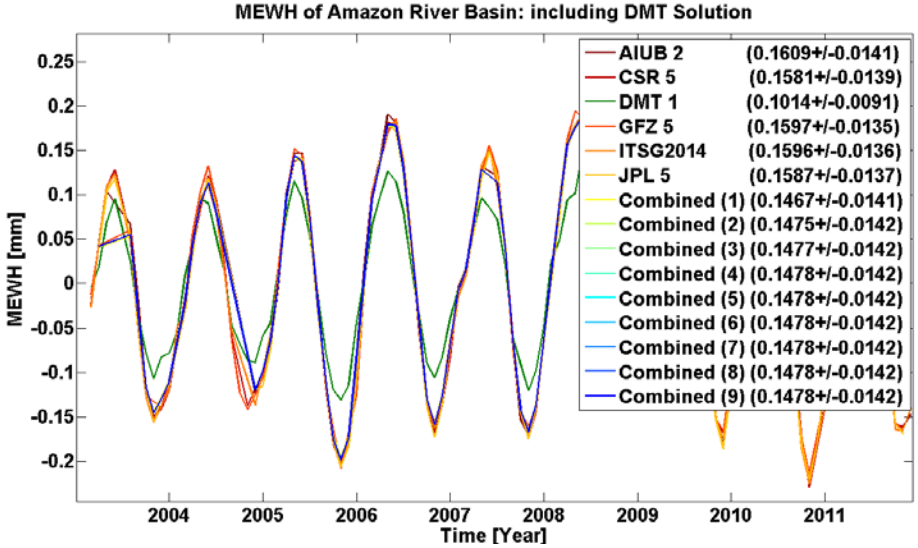

Fig. 3.21: MEWH in the amazon river basin oft he individual solutions and the combination including DMT. Iteration number and corresponding amplitude are given in the legend.

3.2.7 Validation (preliminary results)

As an internal validation (without the use of independent observations) of the combined solutions, the trend of ice mass loss in Antarctica using the individual GRACE monthly solutions and their combination is investigated. For the 27 drainage systems in Antarctica (as defined by the Goddard Ice Altimetry Group: http://icesat4.gsfc.nasa.gov/cryo_data/ant_grn_drainage_systems.php) shown in Fig. 3.22, the ice masses are derived from the MEWH of each drainage system (Fig. 3.23).

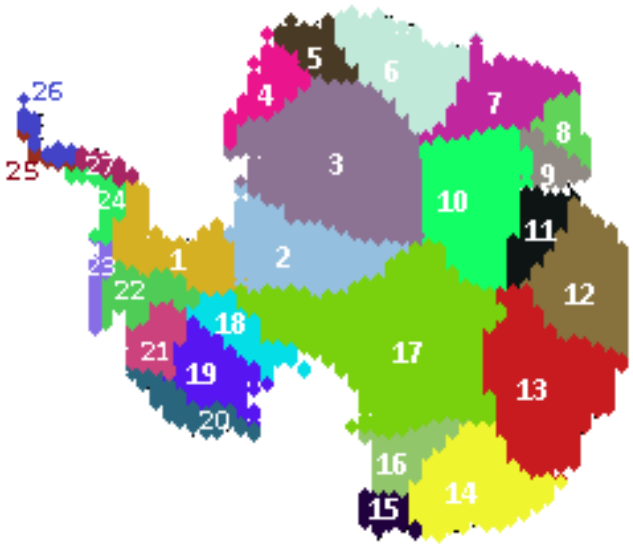

Fig. 3.22: The 27 glacial drainage systems in Antarctica for which ice mass trends are analyzed.

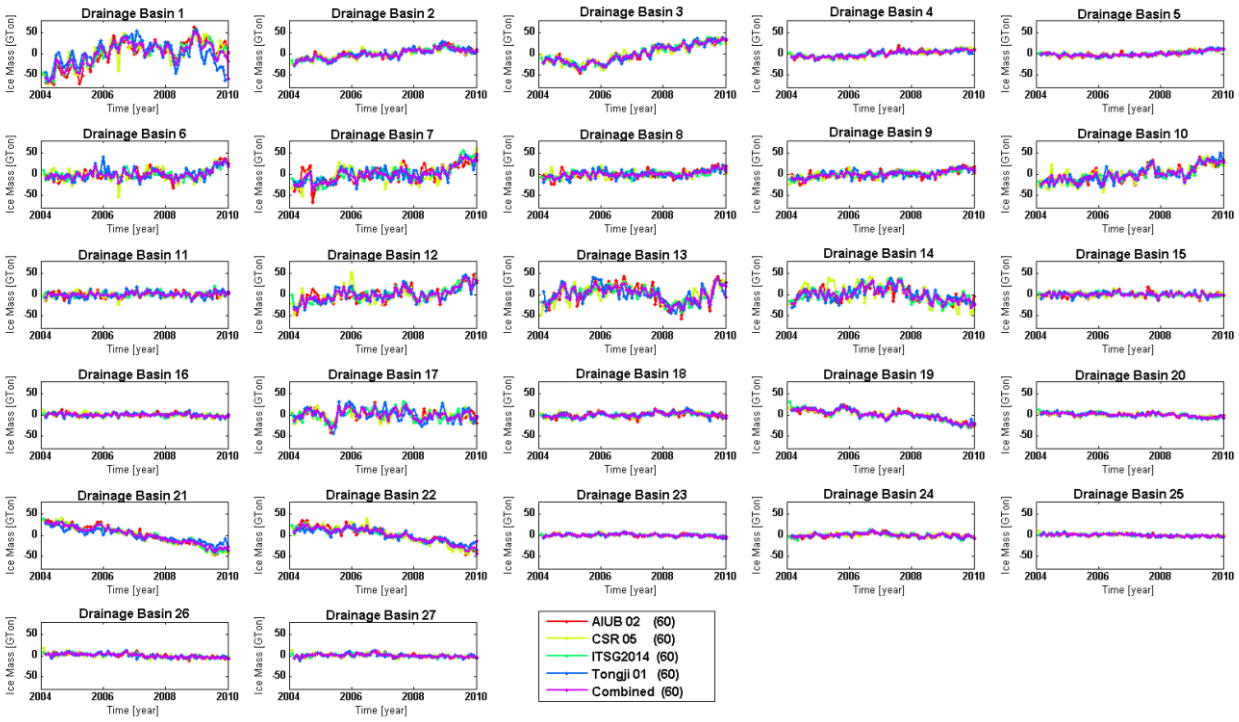

Fig. 3.23: Ice mass changes in the 27 drainage systems in Antarctica.

The ice mass trend for each basin (Fig. 3.24, top) and its formal error (Fig. 3.25, bottom) are estimated as part of a deterministic model containing bias, trend, annual and semi-annual variations. The combined solution (using single weights per month) is less scattered than the individual solutions, as shown by the formal errors, while the size of the trend corresponds well.

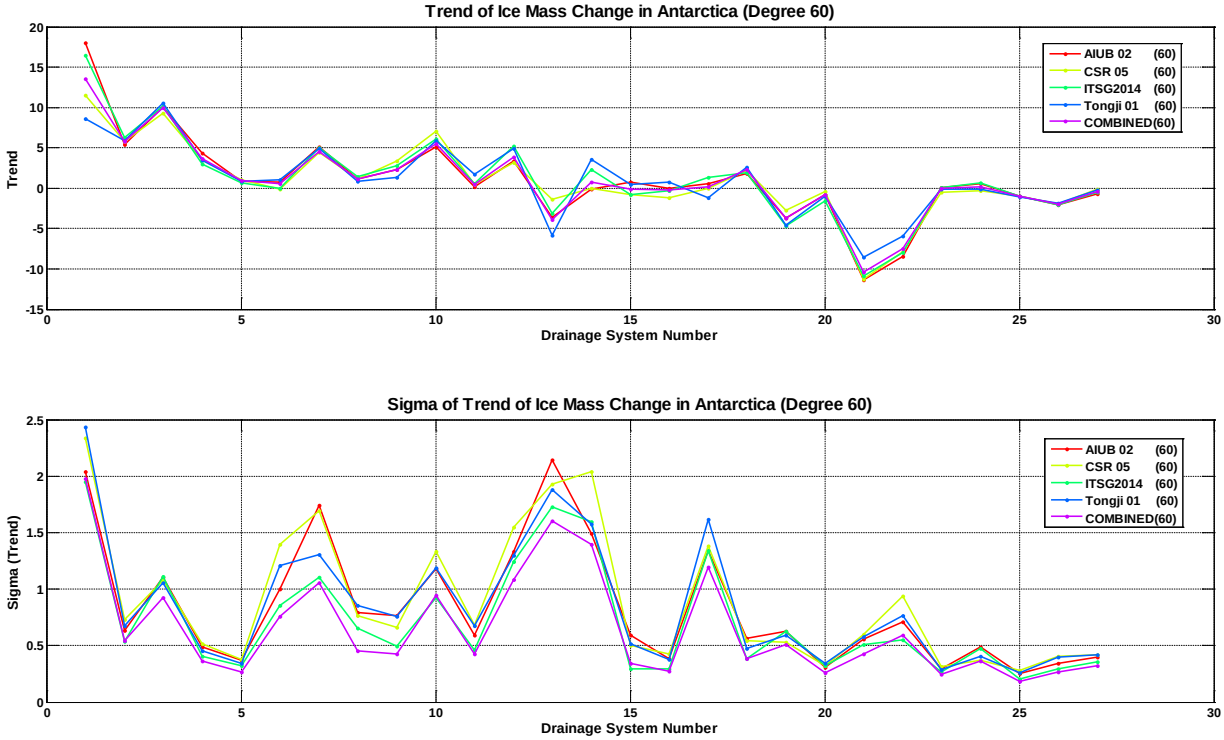

Fig. 3.24: Trend estimate (Gt/a) and formal error (Gt/a) for each of the 24 glacial basins of Antarctica

The ice masses and trends in Figs. 3.24 and 3.25 show the integrated mass effect. No model for snow accumulation or global isostatic adjustment (GIA) has been applied. The uncertainties of these models are much larger than the formal errors of the trend estimates shown above. Besides the internal validation, further external validations of the combined solution are planned in WP3 (T3.5 and T3.6) and Task 4.3 of WP4. External validation results of a first EGSIEM test combination were presented by Horwath et al. (2016).

3.2.8 Recommendation and Plan

As of June 2016, four of the five EGSIEM processing centers (namely CNES, GFZ, TUG and UBERN) are ready to provide improved GRACE monthly gravity fields for the combination and one processing center plans to provide its GRACE monthly gravity field solution in the near future (UL). The EGSIEM also welcomes further processing centers to join the combination service. So hopefully in the near future, there will be not only the newly released monthly solutions by the existing EGSIEM processing centers available for combination, but also the monthly solutions by newly joined processing centers.

All contributions will first undergo the strict quality control as outlined in Sect. 3.2.2 and 3.2.3. Individual monthly solutions or whole time series that fail the quality test will be rejected to avoid any impairment of the combined solution. The selected monthly solutions will be combined using the VCE weighting scheme (Sect. 3.2.4) and will undergo an internal validation for quality control (Sects. 3.2.5 and 3.2.7), before they are validated by comparison with independent observations (T4.3).

After passing the quality control and external validation the combined solutions are provided to the user as spherical harmonic coefficients in ICGEM file format (Fig. 3.25), and in L3 grid format (Sect. 5). The maximum degree and order of the combined monthly solutions will be 90. The sigma C and sigma S will be replaced by weighted standard deviations of the combination and therefore represent formal errors of the combination. The format of the file name will be **egsiem_vv_dd_mm_yyyy.gfc**, where vv is the version/release number, dd is the maximum degree of the solution, mm is the month, and yyyy is the 4-digit year.

```
CMMNT GRACE-only monthly gravity field 2003/03
CMMNT Combined solution provided by EGSIEM project
CMMNT Generated on 21 October 2015 at Astronomical Institute, University of Bern
CMMNT Contact: Y. Jean, yoomin.jean@aiub.unibe.ch
CMMNT Contact: U. Meyer, ulrich.meyer@aiub.unibe.ch
CMMNT Contact: A. Jaeggi, adrian.jaeggi@aiub.unibe.ch
CMMNT Total 5 Contributing Solutions (normalized weight)
CMMNT [1] AIUB RL2  (0.3)
CMMNT [2] CSR  RL5  (0.2)
CMMNT [3] GFZ  RL5  (0.1)
CMMNT [4] ITSG 2014 (0.3)
CMMNT [5] JPL  RL5  (0.1)
CMMNT The EGSIEM Horizon 2020 project, supported by European Commission

begin_of_head ==================================================
product_type                 gravity_field
generating_institute         EGSIEM
modelname                    EGSIEM_01
earth_gravity_constant       0.3986004415E+15
radius                       0.6378136300E+07
max_degree                   90
tide_system                  tide_free
errors                       weighted standard deviations of combination (formal)

key    L    M       C                  S                  sigma C            sigma S
end_of_head ====================================================================================
gfc    0    0  1.000000000000E+00  0.000000000000E+00 0.000000000000E+00 0.000000000000E+00
gfc    1    0  0.000000000000E+00  0.000000000000E+00 0.000000000000E+00 0.000000000000E+00
gfc    1    1  0.000000000000E+00  0.000000000000E+00 0.000000000000E+00 0.000000000000E+00
…
```

Fig. 3.5: Example of EGSIEM combined solution in ICGEM file format.

3.3 References

Bettadpur, S. (2012): UTCSR level-2 processing standards document. Center for Space Research, University of Texas at Austin.

Bruinsma, S., J.-M. Lemoine, R. Biancale, and N. Valès (2010) : CNES/GRGS 10-day gravity field models (release 2) and their evaluation. Advances in Space Research, 45(4): 587–601.

Brunsima et al. (2015): EGSIEM - a new Horizon2020 project to improve accessibility to gravity field products for hydrology. Hydrospace Workshop, Frascati, Italy, 15-17 September, 2015.

Chen, Q., Y. Shen, X. Zhang, H. Hsu, W. Chen, X. Ju, and L. Lou (2015): Monthly gravity field models derived from GRACE level 1b data using a modified short-arc approach. Journal of Geophysical Research: Solid Earth, 120(3): 1804–1819.

Dahle, C., F. Flechtner, Ch. Gruber, D. König, R. König, G. Michalak, and K.-H. Neumayer (2012): GFZ GRACE level-2 processing standards document for level-2 product release 0005, GFZ.

Hofmann-Wellenhof, B., and H. Moritz (2006): Physical Geodesy. Springer-Verlag Wien.

Horwath, M., A. Groh, and the EGSIEM Team (2016): Evaluation of recent GRACE monthly solution series with an ice sheet perspective, EGU General Assembly 2016, Vienna, Austria, 17-22 April, 2016.

Jäggi, A., Y. Jean, U. Meyer, A. Sušnik, M. Weigelt, T. van Dam, Z. Li, F. Flechtner, C. Gruber, A. Güntner, B. Gouweleeuw, T. Mayer-Gürr, A. Kvas, S. Martinis, H. Zwenzer, S. Bruinsma, J.-M. Lemoine, J. Flury, S. Bourgogne, H. Steffen, and M. Horwath (2015): European Gravity Service for Improved Emergency Management - Project Overview and First Results. AGU Fall Meeting 2015, San Francisco, California, 14 - 18 December, 2015.

Jean, Y., U. Meyer, and A. Jäggi (2015a): Combination of GRACE monthly gravity field solutions from different processing centers, EGU General Assembly 2015, Vienna, Austria, 12-17 April, 2015.

Jean, Y., U. Meyer, and A. Jäggi (2015b) : Combination of GRACE monthly gravity field solutions using different weighting schemes. Geodätische Woche 2015 Stuttgart, Germany, 15-17 September, 2015.

Jean, Y., U. Meyer, U., and A. Jäggi (2016) : Simulation Study on Combination of GRACE monthly gravity field solutions. EGU General Assembly 2016 Vienna, Austria 17-22 April, 2016.

Liu, X., P. Ditmar, C. Siemes, D.C. Slobbe, E. Revtova, R. Klees, R. Riva, and Q. Zhao (2010): DEOS mass transport model (DMT-1) based on grace satellite data: methodology and validation. Geophysical Journal International, 181(2): 769–788.

Mayer-Gürr, T., N. Zehentner, B. Klinger, and A. Kvas (2014): ITSG grace2014: a new grace gravity field release computed in Graz. GRACE Science Team Meeting 2014, Potsdam.

Meyer, U., A. Jäggi, Y. Jean, and G. Beutler (2016): AIUB-RL02: an improved time series of monthly gravity fields from grace data. Geophysical Journal International, 205(2): 1196-1207

Tapley, B. D., S. Bettadpur, M. Watkins, and C. Reigber (2004): The gravity recovery and climate experiment: Mission overview and early results. Geophysical Research Letters, 31(9).

Wahr, J., M. Molenaar, and F. Bryan (1998): Time variability of the Earth's gravity field: Hydrological and oceanic effects and their possible detection using GRACE. Journal of Geophysical Research: Solid Earth, 103(B12): 30205–30229.

Watkins, M., T. Gruber, and S. Bettadpur (2000): Science Data System Development Plan. GRACE Project. 327-710.

Watkins, M., and D.-Y. Yuan (2012): JPL Level-2 processing standards document for level-2 product release 05. NASA JPL.

3.4 Appendix to Section 3

3.4.1 C_{20} comparison

The C_{20} coefficients of the individual time series of monthly solutions show large differences (as shown in Fig. 3.4). Even the long-time mean differs considerably between different processing centers. Differences of the mean over time between the individual time-series and the SLR-derived values (published in GRACE TN07 by CSR) are given in Tab. 3.4.

Tab. 3. 4: Mean(C_{20}_Sol) — Mean(C_{20}_CSR)

C20 Difference w.r.t. CSR	
	Degree 60
AIUB - CSR	-7.58E-11
GRGS - CSR	-1.98E-10
ITSG - CSR	-1.77E-11
Tongji - CSR	-8.45E-11

C20 Difference w.r.t. CSR	
	Degree 90
AIUB - CSR	-7.64E-11
GFZ - CSR	1.33E-10
ITSG - CSR	-4.41E-12
JPL - CSR	2.33E-11

3.4.2 Median Absolute Deviation

Median absolute deviation (MAD) is a measure of variability, which is insensitive to the existence of outliers and not affected by the sample size. It is computed as:

$$MAD = median(|X_i - median(X_i)|) \qquad (3.6)$$

with X_i, $i=1, \ldots, n$ the individual members of a sample of size n. To detect outliers, commonly a threshold of three times the MAD is used.

3.4.3 GRACE ground track spacing

The geometry of the ground-tracks of the GRACE satellites determines the maximum resolution of the gravity field produced by the data from the satellites. In certain months, the GRACE satellites inevitably experience resonance-orbits. During these periods the ground-tracks of the GRACE satellites are not dense enough to acquire high-resolution gravity fields without using regularization techniques (Fig. 3.26). Because not all processing centers provide free solutions during times of orbit resonance and because the EGSIEM combination relies on free (un-biased) solutions, periods of orbit resonance lead to gaps in the EGSIEM time series of combined monthly gravity fields.

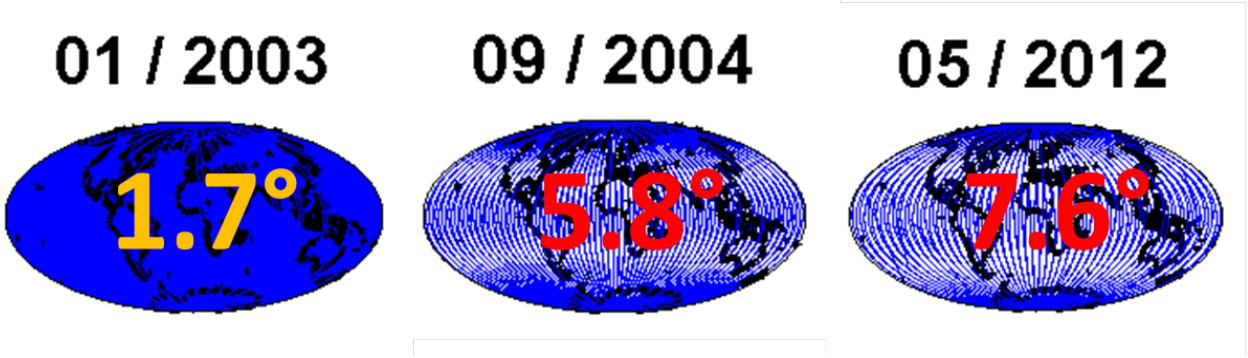

Fig. 3.26: Ground-tracks of GRACE A during three example months. The corresponding maximum longitudinal spacing between the ground tracks is provided for each of the ground-track plots.

In Fig. 3.27 the maximum longitudinal spacing per month between the ground tracks of GRACE A is provided. The maximum resolution of the monthly gravity fields is directly dependent on this spacing. During the 4-day-repeat resonance period in fall 2004 free monthly gravity fields can only be produced up to a maximum order of 60, while during the 3-day-repeat resonance period in spring/summer 2012 the maximum degree is even reduced to order 45.

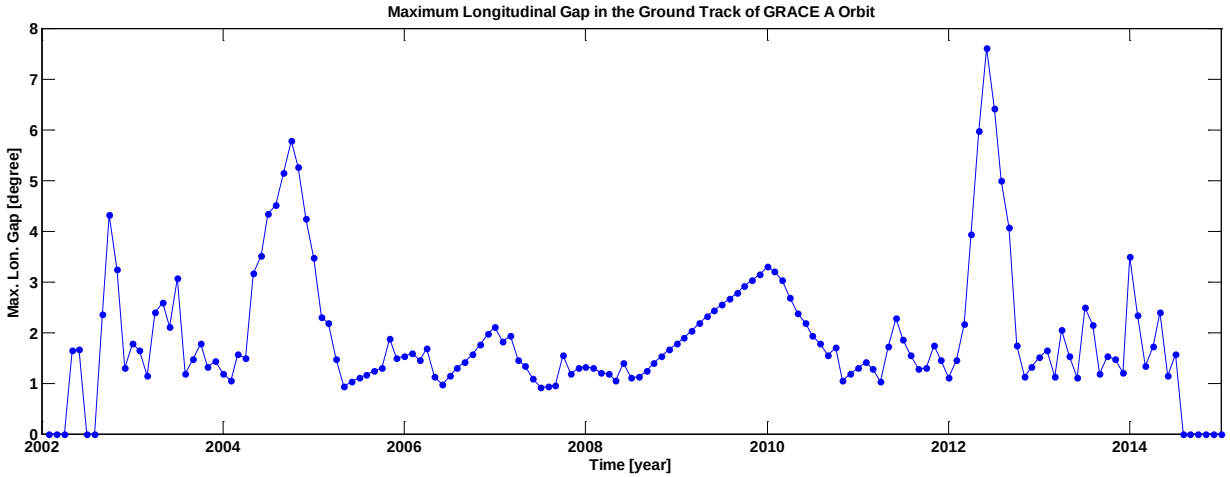

Fig. 3.27: Maximum longitudinal spacing of the ground-tracks of GRACE A.

3.4.4 Sensor Fusion Data

In the GRACE data processing, usually one of the two on-board star cameras on each of the two GRACE satellites is used to determine the satellites' attitude. But in principle it is possible to combine these direct attitude observations with integrated angular accelerations observed by the accelerometers. To date this so-called sensor fusion data is produced and exploited only by ITSG at TU Graz that kindly provided it for test purposes to the EGSIEM consortium. The sensor fusion data has reduced high frequency components compared to the Level-1B data. This results in a much smoother geometrical K-band correction. The geometric K-band corrections included in the Level-1B data and derived from the sensor fusion data are compared in Fig. 3.28 in the time domain (top) and the spectral domain (bottom).

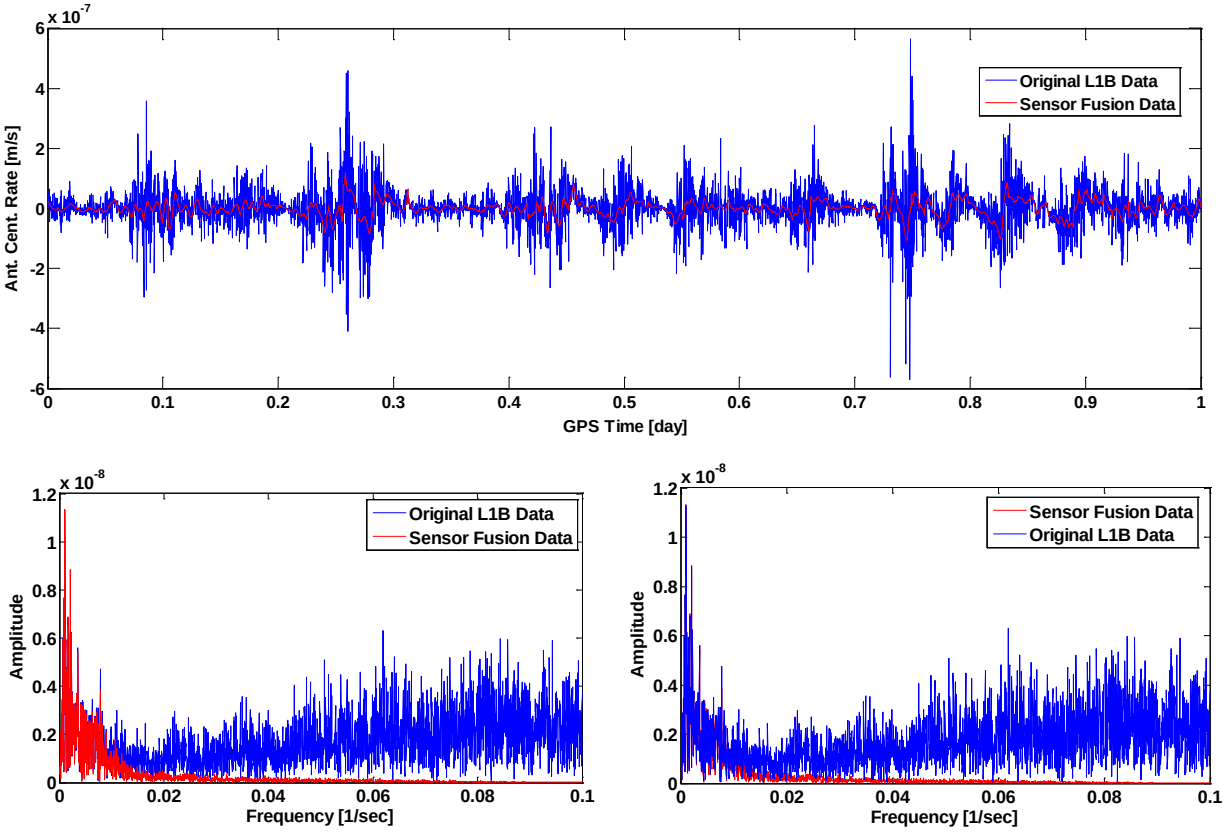

Fig. 3.28: Original L1B geometric K-band correction (blue) and geometric K-band correction derived from sensor fusion data (red) for January 2007, (top) in the spatial domain, (bottom left and right) in the spectral domain (both figures are basically identical; (left) the sensor fusion data is plotted on top, (right) the original data is plotted on top.

To investigate the effect of the sensor fusion data, the AIUB monthly gravity field of January 2007 has been reprocessed using the sensor fusion data provided by ITSG. Figure 3.29 shows the difference between two monthly AIUB solutions using either the geometric K–band correction provided as Level 1B data or the one derived from the sensor fusion data. Mainly zonal terms are affected. This corresponds to the observation that the zonal terms of the monthly ITSG gravity fields are systematically different from the other processing centers (see Fig. 3.9). In view of the reduced high frequency noise in the geometric K-band correction it is very probable that the zonal coefficients of ITSG are better then the zonals of the other processing centers, albeit the difference is rather small.

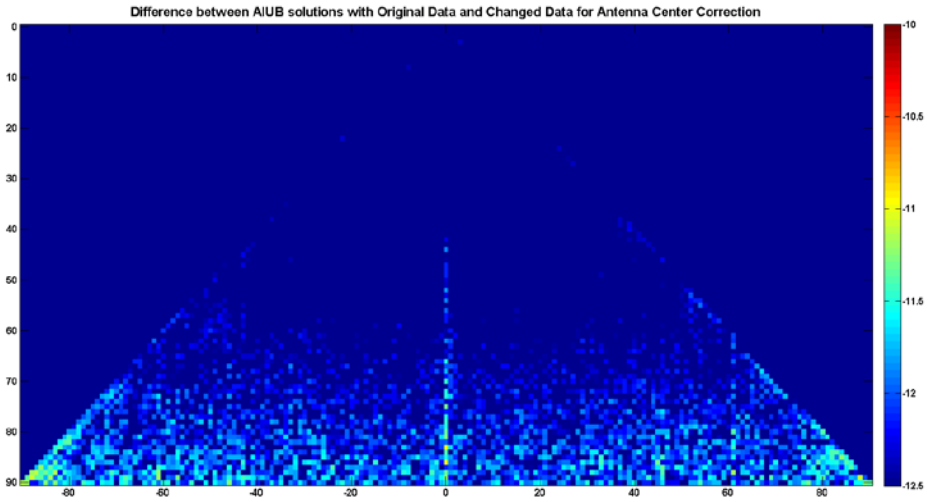

Fig. 3.29: Coefficient-wise differences between two monthly AIUB solutions using either the original L1B geometric K-band correction or the one derived from the sensor fusion data.

4.Combination on Normal Equation Level

4.1 Input

- Monthly normal equations (NEQs) of all contributing ACs, including a priori gravity field coefficients and estimated solutions,
- relative weights (per month and NEQ)

Monthly normal equations: All NEQs are based on common processing standards (D2.1) and are output from the data analysis (T2.3) at the individual ACs. The NEQs consist of

- the a priori gravity coefficients (including the monthly mean of a priori temporal gravity variations): $\mathbf{x_0}$,
- the normal equation vector: $\mathbf{b} = \mathbf{A}^T\mathbf{Pl}$,
- the lower or upper triangle of the normal equation matrix: $\mathbf{N} = \mathbf{A}^T\mathbf{PA}$, and
- the estimates: $\mathbf{x} = \mathbf{x_0} + \mathbf{dx}$.

They include all gravity field coefficients from degree 2 up to degree and order 90. Coefficient C_{00} is fixed to 1, coefficients of degree 1 are fixed to 0 to stay consistent with the reference frame defined in D2.1. Arc- and satellite-specific parameters are pre-eliminated. All gravity field coefficients are free of constraints. Together with the NEQs the following information is provided:

- Earth radius: R_E,
- gravitational constant times Earth's mass: GM_E,
- tide system: zero tide / tide free.

To compute NEQ-statistics further information is given:

- number of parameters: n_{par},
- number of observations: n_{obs},
- weighted square sum of discrepancies O-C (observed minus computed): $\mathbf{l}^T\mathbf{Pl}$.

The number of parameters n_{par} refers to the gravity field coefficients only (not counting the pre-eliminated parameters). The number of observations n_{obs} has to be reduced by the number of pre-eliminated parameters. The estimates x are needed to check the inversion of Nx = b at the combination center for consistency with the individual solutions.

The NEQs are based on GRACE K-Band and GPS phase observations or alternatively kinematic orbit positions. The NEQs are normalized, the relative weighting of the individual observation types is at the choice of the ACs.

Relative weights of NEQs: Relative weights of the individual ACs contributions are defined by the combination on solution level (see Sect. 3). They are normalized per month. They are applied to the combination at normal equation level after the individual NEQs were scaled to equally contribute to the combination.

4.2 File Formats

Normal equations: The NEQs are provided by the individual ACs in Solution INdependent EXchange (SINEX) format (http://www.iers.org/IERS/EN/Organization/AnalysisCoordinator/SinexFormat/sinex.html). SINEX is a standard format for normal equation exchange that is maintained by the International Earth Rotation Service (IERS). For NEQ exchange in the frame of the EGSIEM gravity field combination service the following SINEX blocks and contents are relevant (numbers are given for example only):

FILE/COMMENT

earth_gravity_constant	3.9860044150e+14
radius	6.3781363000e+06
tide_system	zero_tide / tide_free

The lines in this block are copied from the header of the individual solutions in GFC-format.

SOLUTION/STATISTICS

NUMBER OF OBSERVATIONS	540481
NUMBER OF UNKNOWNS	8277
WEIGHTED SQUARE SUM OF O-C	5.1761025e+05

SOLUTION/ESTIMATE

```
1 CN     2 --   0 06:016:43200 ---- 2 -4.84169160788564e-04  1.39923e-11
2 CN     2 --   1 06:016:43200 ---- 2 -3.41480150232469e-10  8.80419e-12
3 SN     2 --   1 06:016:43200 ---- 2  1.46383672520029e-09  8.37504e-12
```

SOLUTION/APRIORI

```
1 CN     2 --   0 06:016:43200 ---- 2 -4.84169219812195e-04
2 CN     2 --   1 06:016:43200 ---- 2 -2.87591948230532e-10
3 SN     2 --   1 06:016:43200 ---- 2  1.47690500410210e-09
```

SOLUTION/NORMAL_EQUATION_VECTOR

```
1 CN     2 --   0 06:016:43200 ---- 2  4.04254781162723e+11
2 CN     2 --   1 06:016:43200 ---- 2 -6.85974043792560e+11
3 SN     2 --   1 06:016:43200 ---- 2  7.71101358350703e+10
```

SOLUTION/NORMAL_EQUATION_MATRIX

Relative weights: The weights consist of only one number per AC and month and are exchange by tabular text files. Missing (or screened out) solutions are marked by a weight of 0.

	AC1	AC2	AC3	AC4
2006/01	W1	W2	0	W4
2006/02	W1	W2	W3	W4
…				

4.3 Weighted combination of normal equations

To develop the tools for SINEX-NEQ handling and combination, preliminary NEQs for one test month January 2006 were provided by TUG, GFZ and UBERN. All results shown in the following are based on these three NEQs. The derived weights do not yet reflect the final accuracy of the individual ACs contributions that will only be available in the operational phase of the EGSIEM combination service, starting in month 19 (July 2016).

The NEQs of the individual ACs are combined at UBERN by the NEQ-inversion and -manipulation tool (Fortran: ADDNEQ2) of the Celestial Mechanics Approach (CMA). Therefore they first are transformed into the Bernese NQ0-format (Fortran-Tool: SNX2NQ0).

4.3.1 Test of consistency

To test the consistency of the NEQ-inversion at AIUB (UBERN) with the inversion at an individual AC the corresponding normal equation in Bernese format is inverted (Fortran-tool: ADDNEQ2). The estimated corrections to the gravity field parameters are added to the a priori gravity model provided by the SOLUTION/APRIORI block of the SINEX-NEQ and the resulting monthly mean gravity field is compared with the individual AC's solution that is extracted from the SOLUTION/ESTIMATE block of the SINEX-NEQ. For the two external SINEX-NEQs from ITSG (TUG) and GFZ the consistency in terms of difference degree variances between the original solutions and the inversion at UBERN is at the level of 10^{-18} to 10^{-19}, 7 to 8 orders of magnitude smaller than the consistency between the ITSG- and the GFZ-solution itself (Fig. 4.1).

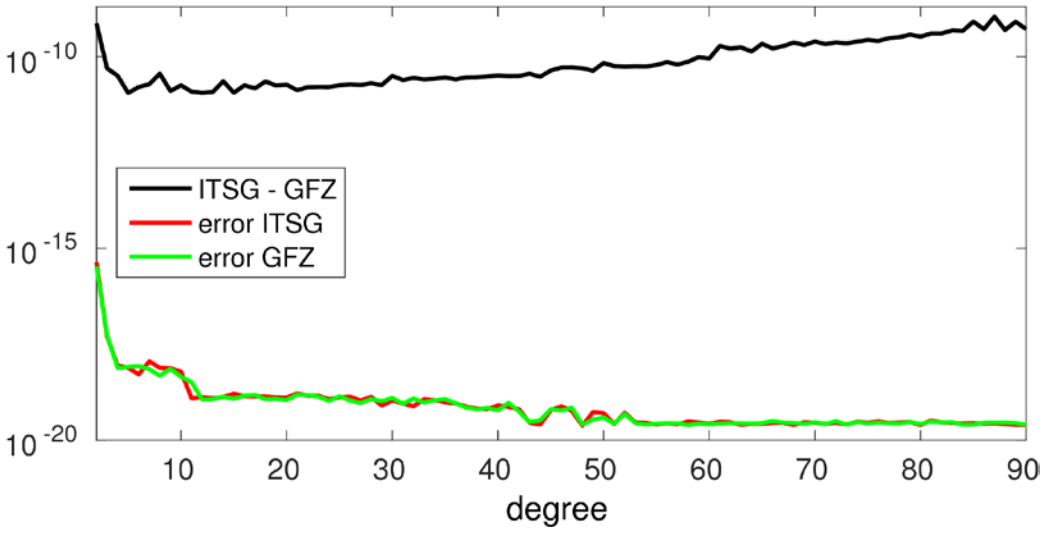

Fig. 4.1: difference degree amplitudes of reconstructed with respect to original solutions.

4.3.2 Transformation to common a priori values

Prior to stacking the NEQs have to be transformed to common Earth radius R_E and GM_E and to common a priori values $\mathbf{x_0}$. The former transformation has to be performed by the tool for the format transformation (SNX2NQ0), because the Earth parameters are not stored in the header of the Bernese NQ0-format and are not available for the NEQ-inversion tool (ADDNEQ2).

Transformation to common R_E and GM_E:
Given are two NEQs

$$\mathbf{N_1}, \mathbf{b_1}, \mathbf{x_{0,1}} \text{ and } \mathbf{N_2}, \mathbf{b_2}, \mathbf{x_{0,2}}$$

that refer to Earth parameters

$$R_1, GM_1 \text{ or } R_2, GM_2.$$

The spherical harmonic coefficients that refer to the two sets of Earth parameters

$$K_{lm,2} = f_l * K_{lm,1}$$

are related by degree-dependant factors (GM_2 and R_2 are considered as reference values)

$$f_l = GM_1/GM_2 * (R_1/R_2)^l.$$

Considering the observation equations

$$\mathbf{y} = \mathbf{A_1 x_1} = \mathbf{A_2 x_2}$$

that refer to these two Earth models we find that the vectors of spherical harmonic coefficients are related via a diagonal matrix **F** with elements

$$F_{ii} = f_l \text{ and } F_{ij} = 0 \text{ for } i \neq j.$$

The dimension of the square matrix **F** corresponds to the number m of estimated parameters **x**, the factors f_l on the main diagonal are sorted corresponding to **x**.

Then the estimates may be written as

$$\mathbf{x_2} = \mathbf{F x_1},$$

and the design matrices as

$$\mathbf{A_2} = \mathbf{A_1 F^{-1}}.$$

The normal equation vectors are consequently scaled by

$$\mathbf{b_2} = \mathbf{F^{-1} b_1},$$

and the normal equation matrices by

$$\mathbf{N_2} = \mathbf{F^{-1} N_1 F^{-1}}.$$

The last incredient of the NEQ to be considered are the a priori values

$$\mathbf{x}_{0,2} = \mathbf{F}\mathbf{x}_{0,1}.$$

To rescale a NEQ with different Earth parameters to a reference set of GM_E and R_E, only the corresponding matrix **F** has to be set up and applied to $\mathbf{x}_0$, **b** and **N**. **F** will always be close to the identity matrix. The effect of the transformation to common Earth parameters is limited mainly to degree 2 coefficients.

Transformation to common $\mathbf{x}_0$:
Given are two NEQs

$$\mathbf{N}_1, \mathbf{b}_1, \mathbf{x}_{01} \text{ and } \mathbf{N}_2, \mathbf{b}_2, \mathbf{x}_{02}$$

with different a priori values

$$d\mathbf{x}_0 = \mathbf{x}_{01} - \mathbf{x}_{02}.$$

The second NEQ shall be transformed to the a priori values of the first NEQ

$$\mathbf{x}_{02}' = \mathbf{x}_{01}.$$

According to Brockmann (1997) the normal equation vector has to be adapted

$$\mathbf{b}_2' = \mathbf{b}_2 - \mathbf{N}_2 d\mathbf{x}_0,$$

while the normal equation matrix remains unchanged

$$\mathbf{N}_2' = \mathbf{N}_2.$$

Also the weighted square sum of O – C has to be corrected (for statistics only)

$$\mathbf{l}_2'^{T}\mathbf{P}_2\mathbf{l}_2' = \mathbf{l}_2^{T}\mathbf{P}_2\mathbf{l}_2 - 2\mathbf{b}_2 d\mathbf{x}_0 + d\mathbf{x}_0^{T}\mathbf{N}_2 d\mathbf{x}_0.$$

4.3.3 Weights based on variance factors

A classical approach to derive weights for normal equation combination is to compute them by the ratio of a priori and a posteriori variance factor: $w = S_0 / \hat{S}_0$, with S_0 the a priori (in case of normalized NEQs: $S_0 = 1$) and $\hat{S}_0$ the a posteriori variance factor. The a posteriori variance factor tells us how well the observational model fits the observations. In general the noise model (as part of the observational model) is optimistic, leading to optimistic formal errors and resulting in an a posteriori variance factor $\hat{S}_0 < S_0$ and correspondingly a weight $w > 1$ of the NEQ.

The a posteriori variance factor is computed by the weighted sum of squares of post fit residuals divided by the degrees of freedom

$$\hat{S}_0 = \mathbf{v}^T\mathbf{P}\mathbf{v} / (n_{obs} - n_{par}),$$

with $\mathbf{v}$ the vector of post fit residuals and $\mathbf{P}$ the weight matrix. The weighted square sum of residuals can be computed by

$$\mathbf{v}^T\mathbf{P}\mathbf{v} = \mathbf{l}^T\mathbf{P}\mathbf{l} - \mathbf{d}\mathbf{x}^T\mathbf{b}.$$

The NEQs provided by the different ACs are based on different observation types:

- GPS phases (GPS),
- kinematic orbit positions (POS), and
- K-Band range-rates (KRR)

at different sampling rates (5 s, 30 s, or 300 s), using different screening criteria. This leads to very different numbers of observations, for the three example NEQs they are:

- ITSG: 540481 (300 s POS, 5 s KRR)
- AIUB: 1016763 (30 s POS, 5 s KRR)
- GFZ: 2691802 (30 s GPS, 5 s KRR)

The number of parameters 8277 is the same for all three example NEQs, corresponding to the number of all gravity field coefficients from degrees 2 to 90 (degrees 0 and 1 are fixed to 1 and 0, respectively).

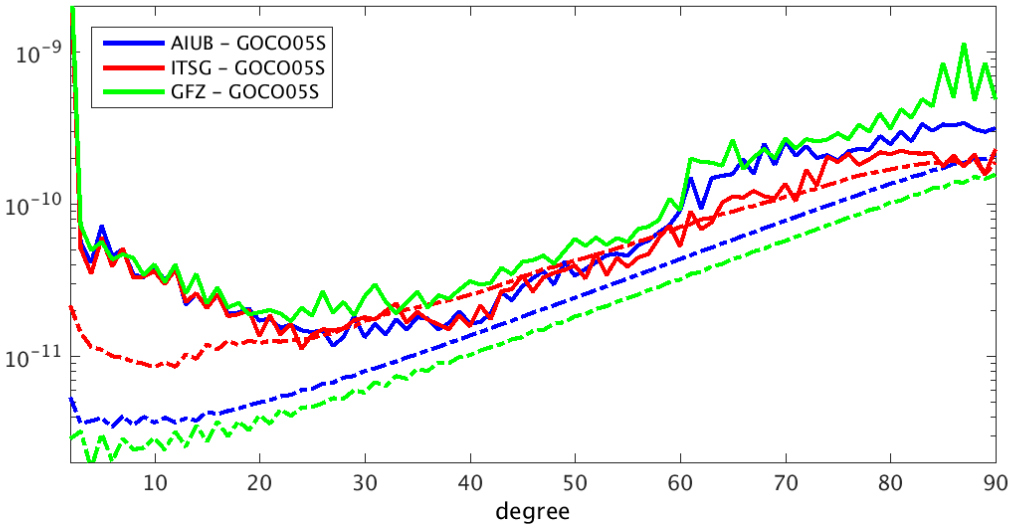

Fig. 4.2: Difference degree amplitudes of individual monthly solutions Jan. 2006 with respect to the static field GOCO05S (reference epoch 01/01/2008) and degree variances of formal errors.

The noise models applied by the different approaches are very different, resulting in realistic formal errors in case of ITSG and optimistic formal errors in case of GFZ and AIUB (as shown in Fig. 4.2, where for the noise-dominated degrees 30-90 the formal errors of ITSG match the actual differences with respect to the superior static reference model GOCO05S, while in case of GFZ and AIUB the formal errors are too small; the low degrees up to 30 are dominated by signal and are therefore not representative for the actual noise level of the coefficients).

The corresponding a posteriori variance factors and resulting weights are:

- ITSG: $\hat{S}_0 = 0.93$, W = 1.08
- GFZ: $\hat{S}_0 = 0.77$, W = 1.30
- AIUB: $\hat{S}_0 = 0.16$, W = 6.25

thus reflecting the different choice of observations and the parametrization / noise model applied by the different ACs. ITSG is punished for its empirical noise model that is leading to realistically large formal errors (a posteriori variance factor close to 1). Application of the derived weights in the combination does not lead to a fair impact of the individual NEQs to the combined solution that reflects the consistency of the individual solutions (see Fig. 4.4), but to an unrealistically small contribution of ITSG that is reflected by large differences between the individual ITSG solution and the combined solution (Fig. 4.3).

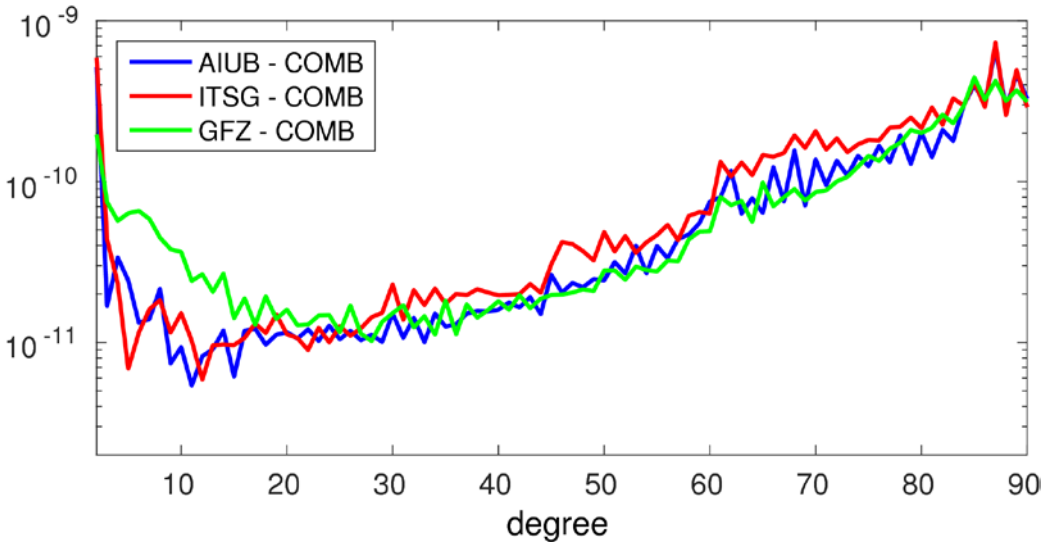

Fig. 4.3: Difference degree amplitudes between individual solutions and combined solution. ITSG shows larger discrepancies (corresponding to smaller contribution) at medium to high degree. The large discrepancies of GFZ at low degrees are not yet explained.

4.3.4 Comparison of individual solutions

To know what to expect from the combined solution first the individual solutions shall be compared. Pairwise difference degree amplitudes (Fig. 4.4) show that the example solutions from UBERN and TUG are more consistent among each other than to the example solution of GFZ. It therefore can be expected that they should also be more consistent with the combined solution of all three NEQs.

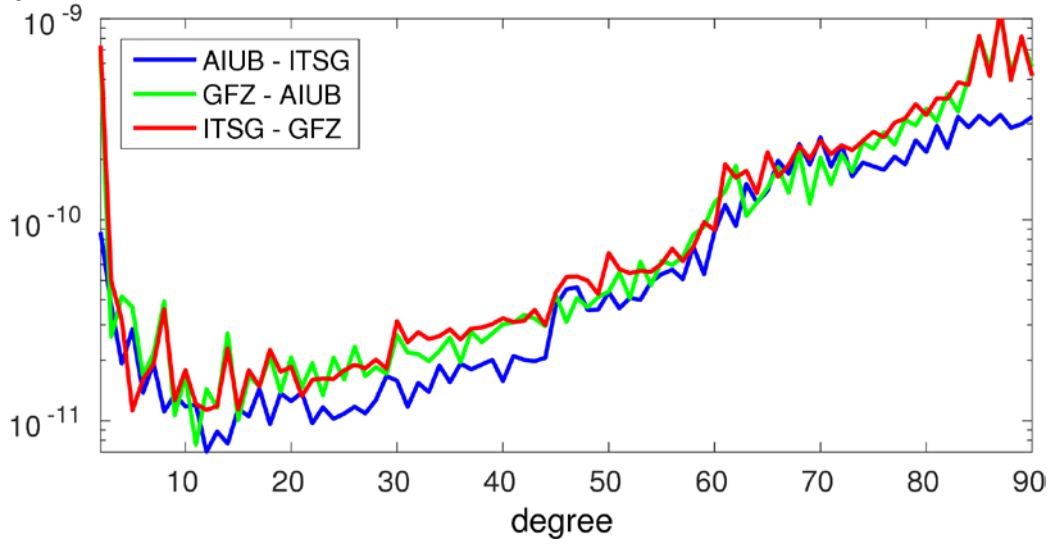

Fig. 4.4: pairwise difference degree amplitudes oft the individual solutions corresponding to the three example NEQs of GFZ, ITSG (TUG) and AIUB (UBERN).

Important characteristics of a NEQ and the corresponding gravity field solution are the formal errors of the gravity field coefficients (Fig. 4.5).

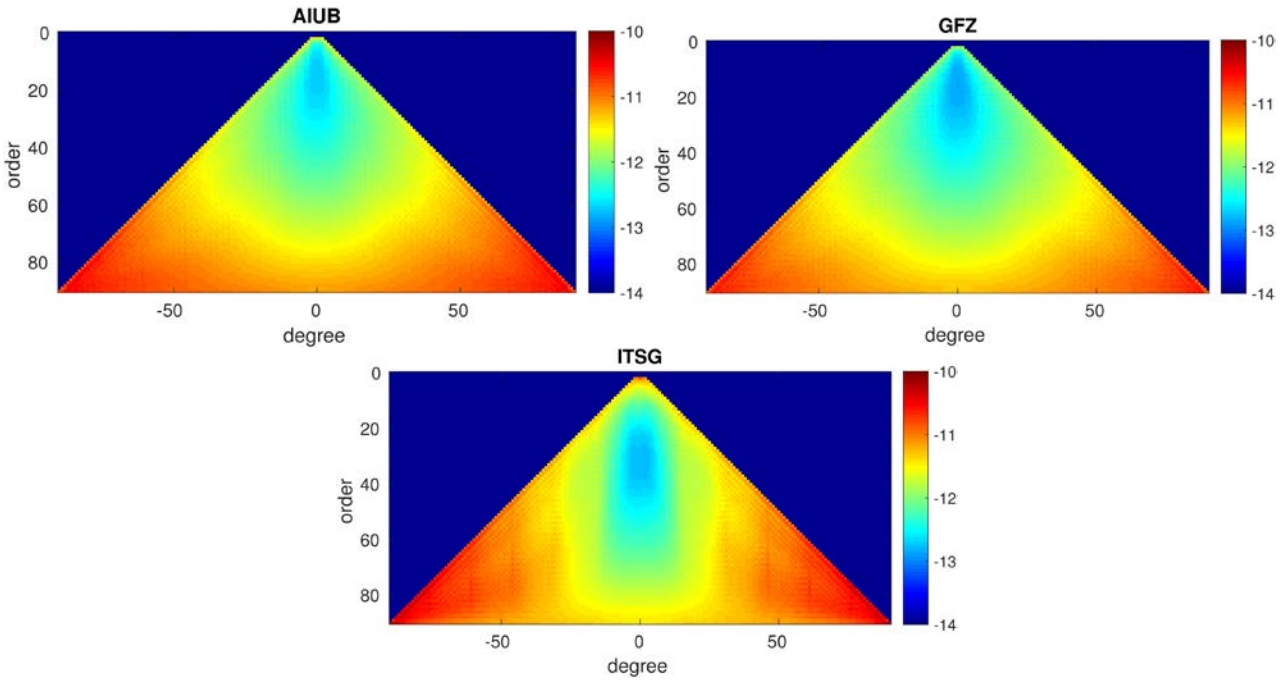

Fig. 4.5: formal errors of the spherical harmonic coefficients (left S-, right C-coefficients) corresponding to the three example NEQs. Top left: AIUB, top right: GFZ, bottom: ITSG.

Weakly determined coefficients get large formal errors and will contribute less to a combined solution than strongly determined coefficients with small formal errors. The formal errors reflect not only the observation geometry (that is the same for all ACs), but also the parametrization and noise model of the individual approaches at the different ACs. It therefore can be expected that the formal errors vary considerably between ACs. Unlike the solutions the formal errors are more consistent between GFZ and AIUB, while the formal errors of ITSG reflect the impact of ITSG's empirical noise model.

4.3.5 Empirical weights for equal contribution of all NEQs

To reach equal impact of the individual NEQs on the combined solution, pairwise combinations are computed and empirical weights are determined iteratively until both individual NEQs contribute equally to the combination. Only the noise-dominated part of the spherical harmonic spectrum (> degree 30) is used to derive the empirical weights (see Figs. 4.6, 4.7 and 4.8).

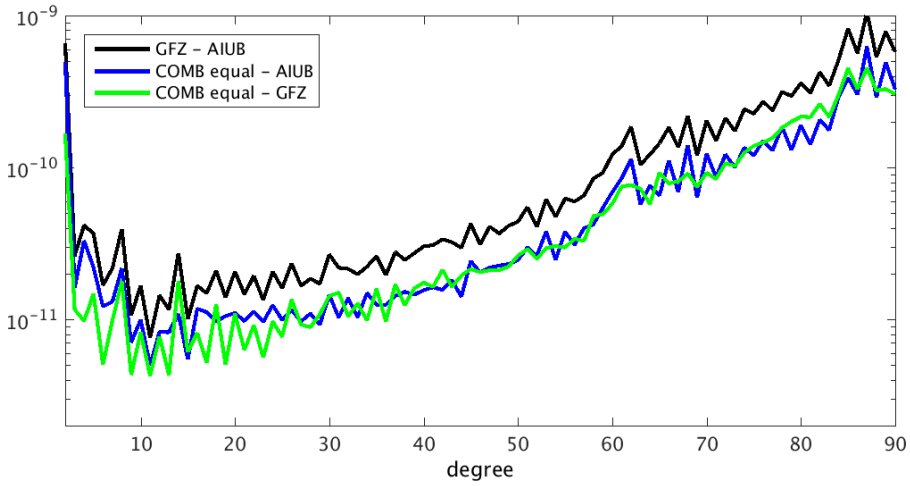

Fig. 4.6: difference degree amplitudes between individual solutions of GFZ and AIUB and between individual and combined solution.

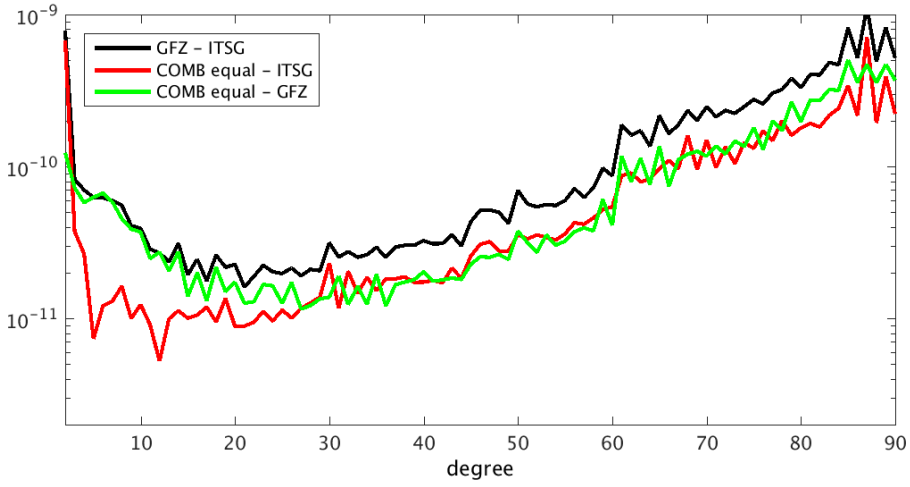

Fig. 4.7: difference degree amplitudes between individual solutions of GFZ and ITSG and between individual and combined solution.

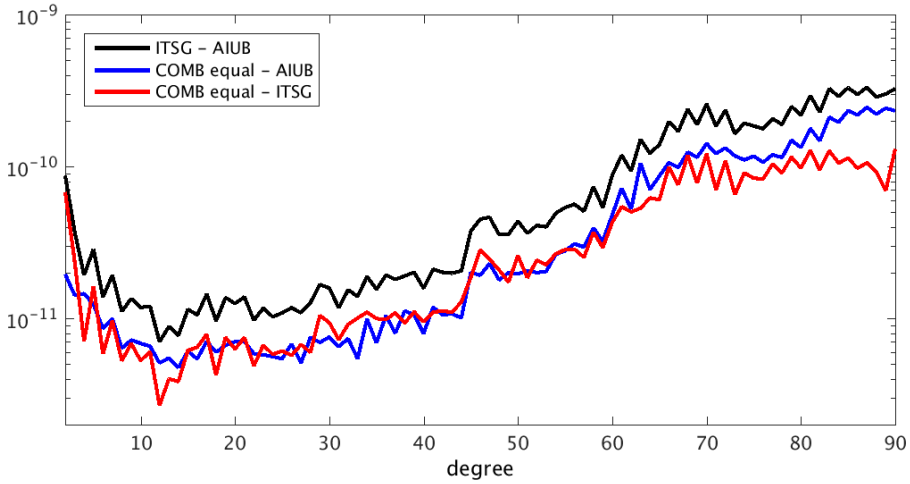

Fig. 4.8: difference degree amplitudes between individual solutions of ITSG and AIUB and between individual and combined solution.

The derived empirical weights are

- GFZ: 1
- ITSG: 5
- AIUB: 6.25

These weights are based on the assumption that all three NEQs have similar noise levels and should contribute equally to the combination. Fig. 4.9 shows the differences between the individual solutions and the combined solution of all three NEQs derived using these empirical weights. As can be expected the combination now is dominated by the two more consistent solutions from ITSG and AIUB. The individual solution of GFZ exhibits the biggest discrepancies to the combined solution (compare to Fig. 4.2).

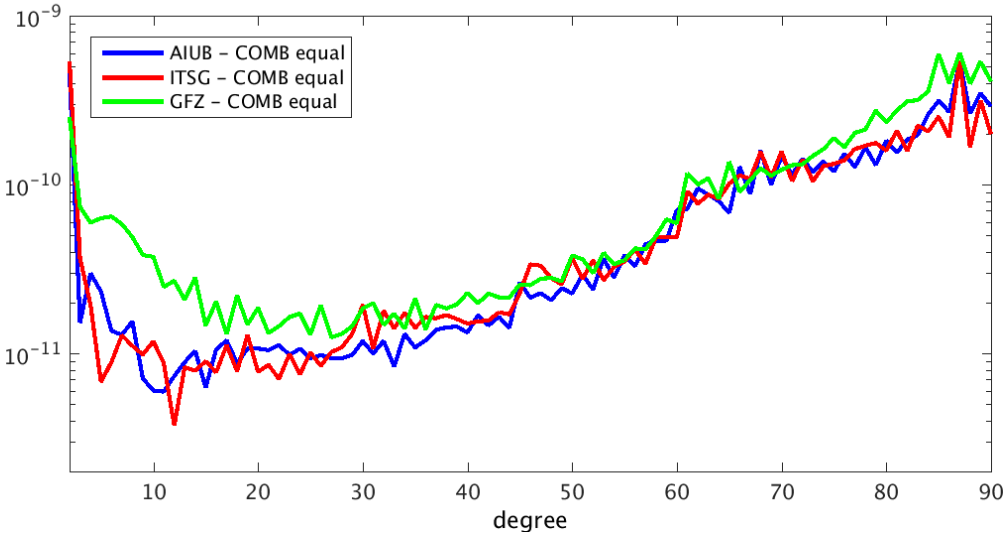

Fig. 4.9: difference degree amplitudes between all individual solutions and the combined solution of all three NEQs applying the empirical weights.

As soon as more NEQs become available from the ACs the pairwise comparison will be augmented / replaced by a leave-one-out scheme as discussed in Lerch (1989).

4.3.6 Contribution analysis

Instead of relying on the comparison of individual and combined solutions to derive relative weights one may directly study the contribution of the individual NEQs by the tools of contribution analysis.

The combined normal equation matrix is computed by stacking (adding up) all individual normal equation matrices

$$\mathbf{N} = \Sigma_i^n w_i \mathbf{N}_i$$

with n the number of normal equations, $\mathbf{N}_i$ the individual stacked normal equation and w_i the relative weight of $\mathbf{N}_i$. The coefficient wise contribution numbers $r_{klm,i}$ (k = 1,2 for C or S coefficients, l and m the degree and order) for normal equation $\mathbf{N}_i$ are the diagonal elements of the resolution matrix

$$\mathbf{R}_i = \mathbf{N}^{-1} w_i \mathbf{N}_i.$$

With normalized weights w_i they add up to 1 per coefficient

$$\Sigma_i^n r_{klm,i} = 1.$$

The coefficient-wise contribution per NEQ is visualized in Figs. 4.10 to 4.12 for the weighting schemes discussed above.

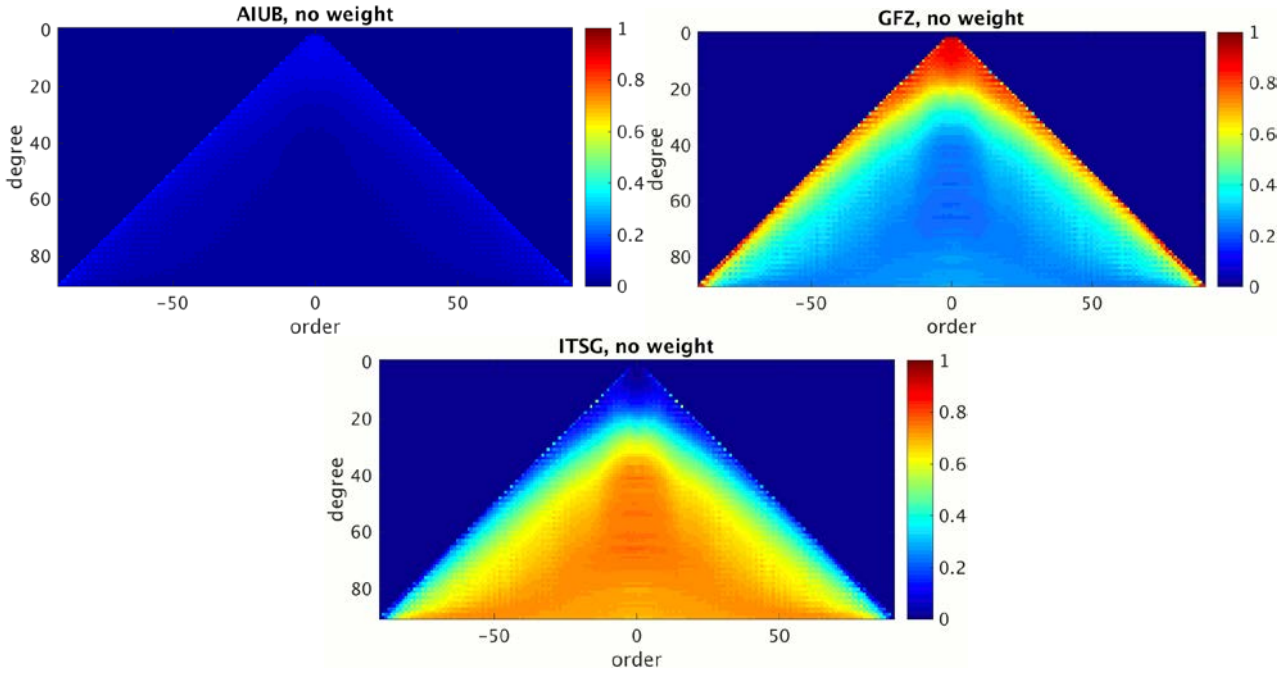

Fig. 4.10: coefficient wise contribution of individual NEQs if no relative weighting is applied.

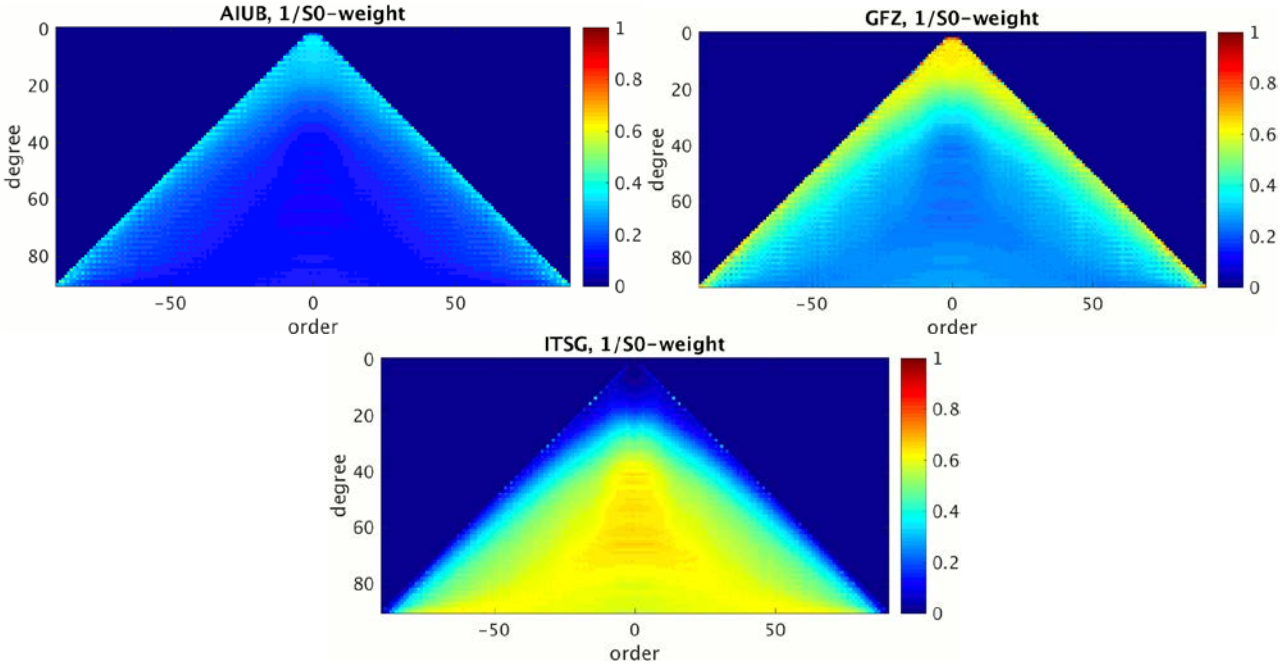

Fig. 4.11: coefficient wise contribution of individual NEQs if variance factors are used for relative weighting.

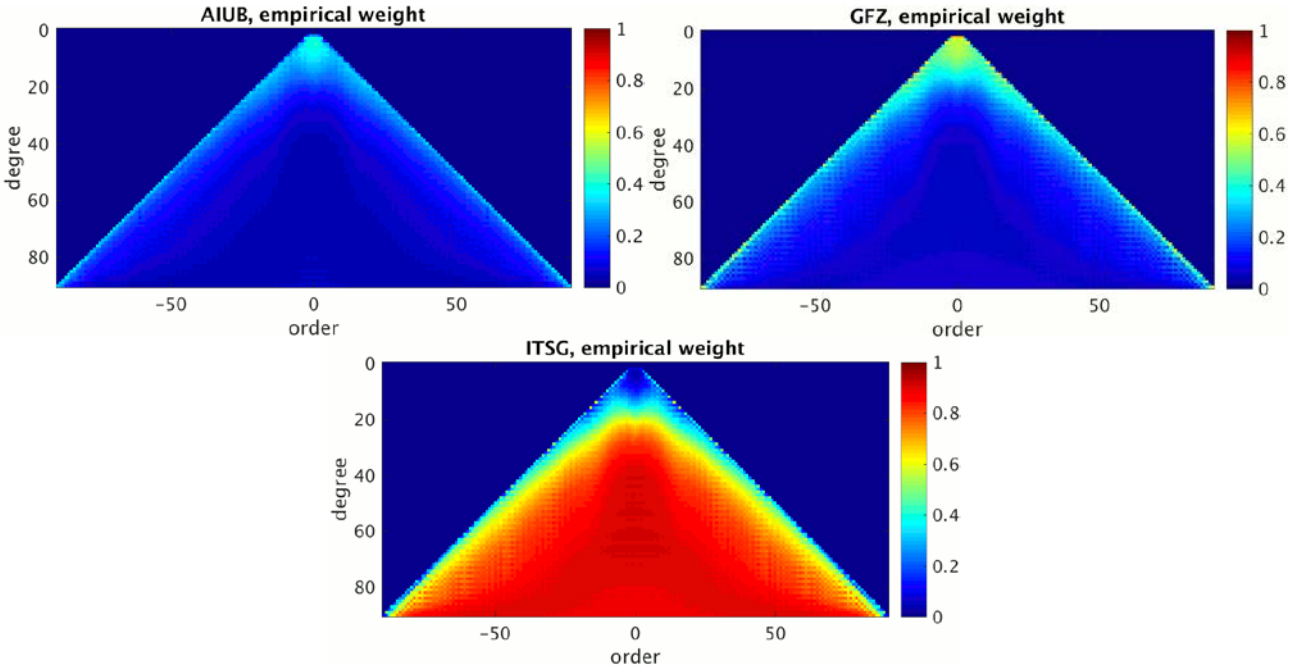

Fig. 4.12: coefficient wise contribution of individual NEQs if empirical weights are applied.

For comparison with the difference degree amplitudes shown in Sect. 4.3.3 to 4.3.5 we can also compute degree variances of the coefficient-wise contributions or the mean contribution per degree (Fig. 4.13). The figures illustrate that the contribution analysis is not in agreement with the results of the pairwise comparison performed in Sect. 4.3.5 and that most probably a degree specific weighting would be appropriate. Unless more NEQs become available from the ACs to perform further tests, the NEQ combination will rely on the weights derived by the pairwise comparison.

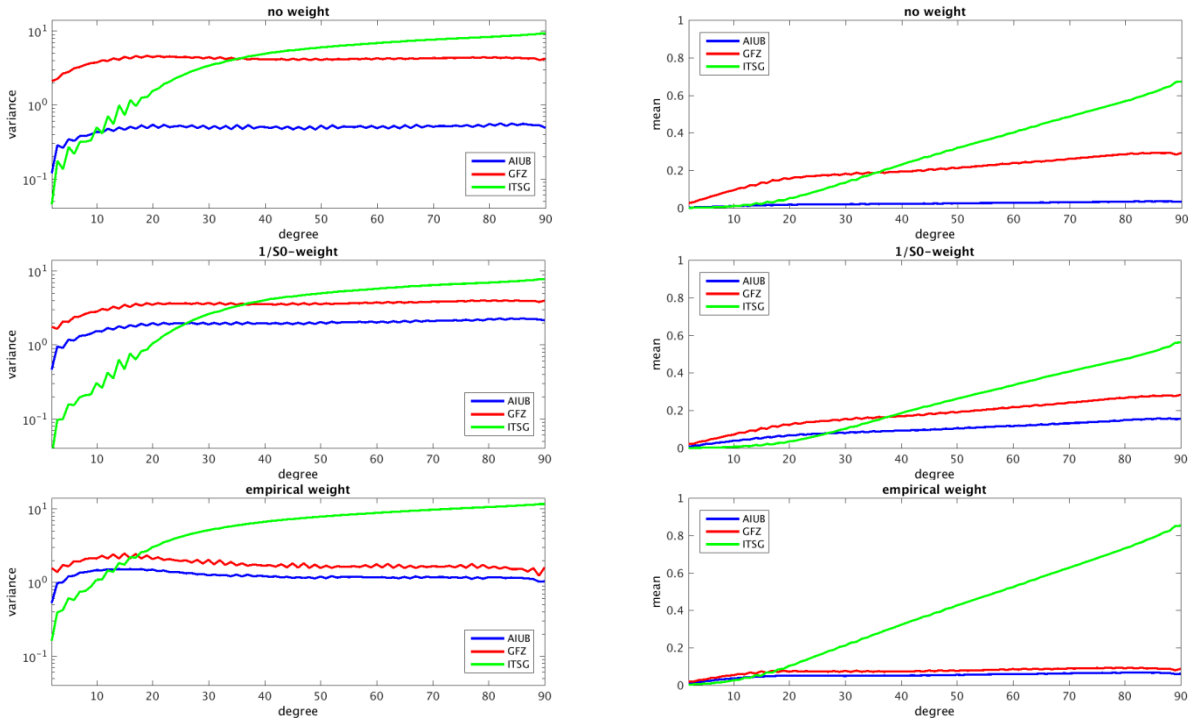

Fig. 4.13: degree variances of contributions (left) and mean contribution per degree (right) of individual NEQs to combination. Top row: no relative weights, middle row: relative weights from variance factors, bottom row: empirical weights that lead to comparable contribution according to pairwise comparisons.

4.3.7 Weights derived on solution level

Applying the empirical weights derived in Sect. 4.3.5 we achieve a combination where all three NEQs contribute approximately equally to the solution (corresponding to the assumption of equal noise levels). But from the combination at solution level (Sect. 3) we know that noise levels of the individual solutions are far from identical.

Because the formal errors and consequently the contribution analysis do not represent the true error levels for all NEQs, we rely on weights that are derived iteratively on solution level by variance component estimation, as described in Sect. 3.2.4. For the three example solutions for January 2006 the weights per iteration are shown in Fig. 4.14. The final weights are

- GFZ: 0.09, scaled to 1
- ITSG: 0.40, scaled to 4.44
- AIUB: 0.51, scaled to 5.67.

They are scaled so that the weight for GFZ again corresponds to 1 for ease of interpretation.

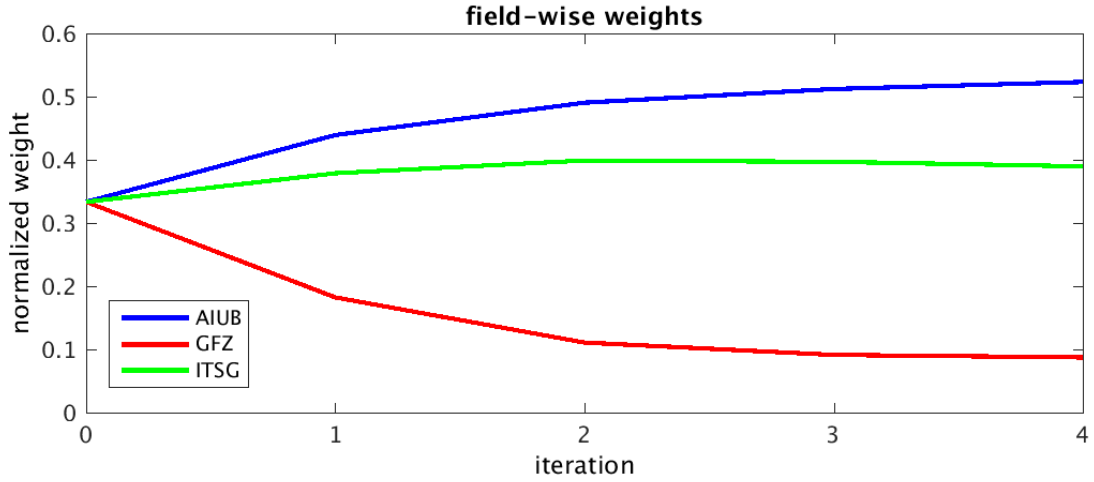

Fig. 4.14: normalized weights oft the three individual solutions derived iteratively by variance component estimation.

These weights are multiplied with the empirical weights derived in Sect. 4.3.5, resulting in the final weights of the combination

- GFZ: 1 * 1 = 1
- ITSG: 5 * 4.44 = 22.20
- AIUB: 6.25 * 5.67 = 35.44.

Note that the first factor accounts for the different processing strategies (observation type and sampling, stochastic parametrization and noise model), while the second one reflects the noise level of the individual solutions derived by comparison to their mean (on solution level). So only the second factor is a quality indicator, while the first one is a technical necessity to make the NEQs comparable.

4.3.8 Quality control

To assess the quality of the combined solutions we cannot rely on the a posteriori variance factor

- $1/S_0$-weighting: $\hat{S}_0 = 1.01$
- empirical weighting: $\hat{S}_0 = 1.33$
- empirical * noise-dependent weighting: $\hat{S}_0 = 4.48$,

because it mainly reflects the consistency based on the formal errors of the individual NEQs (and is 1 per definition if we use the a posteriori variance factors determined in Sect. 4.3.3 for weighting).

Instead we rely on the quality measures described in Sect. 3, namely the weighted standard deviation of the short periodic variability (in equivalent water height (EWH)) over the oceans, which are

- $1/S_0$-weighting: wSTD = 9.5 mm of EWH
- empirical weighting: wSTD = 7.5 mm of EWH
- empirical * noise-dependent weighting: wSTD = 5.9 mm of EWH

for the three test combinations.

Additionally we compute coefficient-wise anomalies by subtraction of coefficient-wise deterministic models consisting of bias, scale, annual and semi-annual variations (the models were defined by evaluation of the time-series of solutions analyzed in Sect. 3). The degree variances of the anomalies, evaluated up to order 29, are shown in Fig. 4.15 for the three different combined solutions.

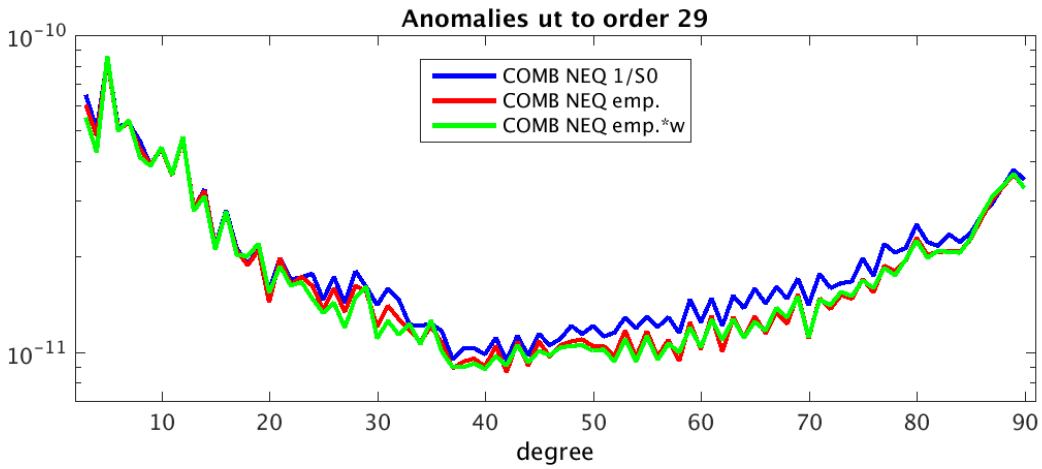

Fig. 4.15: degree variances, based on coefficient wise anomalies up to order 29, of the three combined solutions.

While the anomalies are consistent for the low degrees < 20 that are dominated by non-periodic signal, the anomalies of medium to high degree that are dominated by noise show a clear advantage of the combinations based on the weights derived in Sect. 4.3.5, and a small improvement if finally the weights derived on solution level are added.

The degree variances of the formal errors of the combined solutions are provided in Fig. 4.16, either for all orders (dotted), or limited to orders 0 to 29 (dashed). Again a significant improvement is visible after application of the weights derived in Sect. 4.3.5, and a small further improvements by multiplication with the weights based on comparisons on solution level (Sect. 4.3.7).

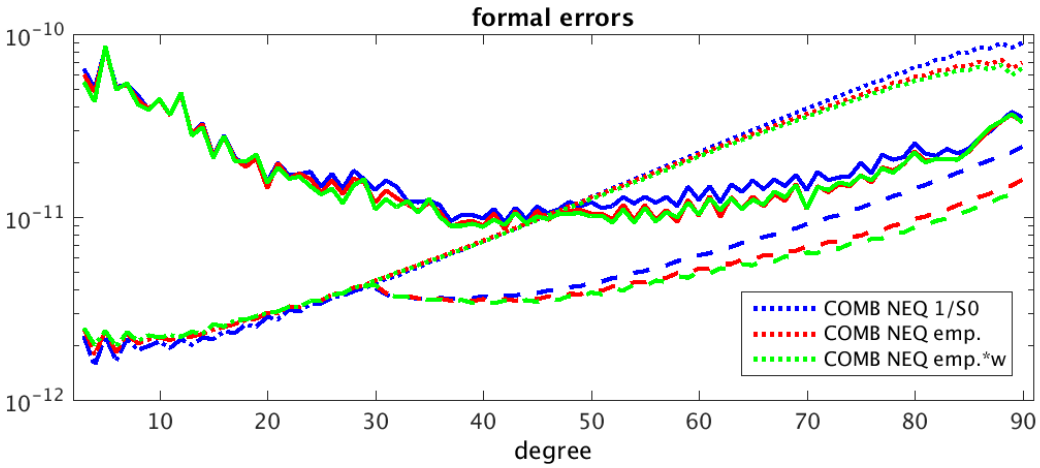

Fig. 4.16: degree variances of anomalies up to order 29 (solid lines), of formal errors of all orders (dotted lines) and of formal errors limited to orders 0 to 29 (dashed lines).

The comparison of the best combination on NEQ-level with the three individual solutions and the combination on solution level is provided in Fig. 4.17. The comparison with the individual solutions uncovers the problem of one dominant solution (ITSG, green) that is not outperformed by the combination on solution level (magenta) throughout all spherical harmonic degrees. The problem is solved in this case by the combination on normal equation level (black) but with the statistically very poor basis of only three NEQs in one example month this is not yet a save conclusion.

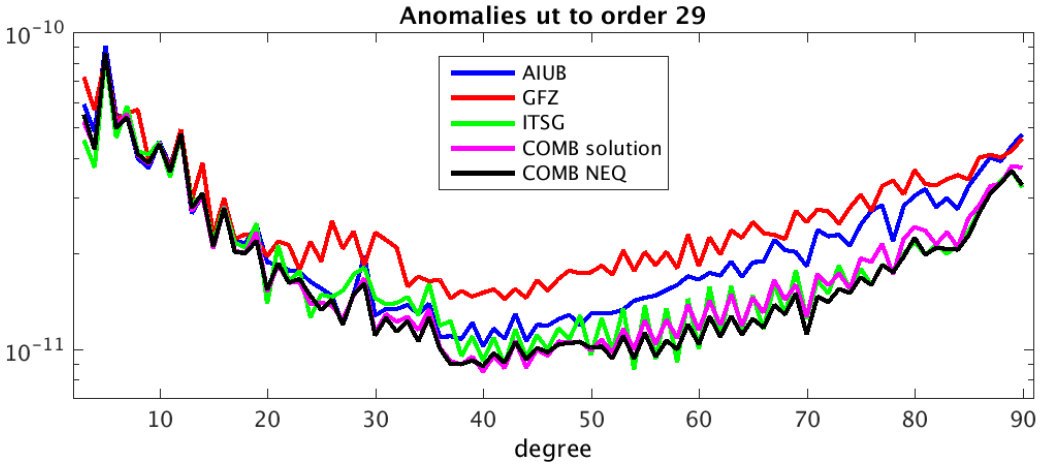

Fig. 4.17: degree variances, based on coefficient wise anomalies up to order 29, of the three individual solutions, the combination on solution level and the final combination on NEQ level.

4.4 References

Brockman, E. (1997): Combination of Solutions for Geodetic and Geodynamic Applications of the Global Positioning System (GPS). Geodätisch-Geophysikalische Arbeiten in der Schweiz (55), Schweizerische Geodätische Kommission, Zürich, Switzerland.

Lerch, F.J. (1989): Optimum Data Weighting and Error Calibration for Estimation of Gravitational Parameters. NASA Technical Memorandum 100737, Goddard Space Flight Center, Greenbelt, Maryland.

5.Level-3 Products

5.1 General

The Level-2 monthly gravity field products derived in EGSIEM, either as individual solutions of the different Analysis Centers (WP2) or the corresponding combined solutions (WP4) are provided in terms of spherical harmonic (SH) coefficients. These coefficients have to be post-processed in order to get rid of artefacts due to increasing noise with increasing degree of the SH solution which is e.g. visible in the spatial domain as north-south orientated striping. Also dedicated SH coefficients have to be substituted (C_{20}) or added (degree 1) to the SH expansion as they are poorly or even cannot be determined by GRACE and GRACE-FO. Additionally, geophysical signals, which were not taken into account during Level-2 processing, such as Global Isostatic Adjustment (GIA), have to be considered. The result of this postprocessing is called Level-3 product and is a ready-to-use user-friendly global 1°x1° grid in terms of equivalent water heights (EWH) provided in standard Ascii or Binary data formats, e.g. netCDF (https://www.unidata.ucar.edu/software/netcdf/). The Level-3 data will be freely accessible using the GRACE plotter interface.

It is planned to provide these Level-3 products in a first step as a single global grid with predefined standards till end of October 2016 (labelled Level-3.1 in the following) and in a second step till June 2017, within the development of the GRACE-FO Science Data System, as additional individual grids for applications in land hydrology, oceanography, glaciology in Polar regions (Antarctica and Greenland) and (TBC) also for Solid Earth applications (labelled Level-3.2 in the following).

In the following the different necessary Level-3 processing steps are described in detail.

5.2 Filters, scaling factors and anti-leakage basin masks

For the generation of user-friendly GRACE/GRACE-FO Level-3 products an appropriate filtering of the Level-2 products is required. This filter has to be applied during the SH synthesis in order to generate EWH grids. A perfect filter would remove the anisotropic north-south stripes, due to correlations between specific spectral orders of the SH coefficients, and at the same time would leave all geophysical signals unaffected. The origin of these correlations lies most likely in the orbit geometry and related observation sampling.

Such a perfect filter is hard to implement in reality. The widely used filter tools for GRACE solutions are of two types: isotropic (e.g. Gaussian smoothing) or anisotropic (e.g Swenson & Wahr (2006) or DDK (Kusche 2007) filter). These filter methods have been implemented at GFZ and have been applied to GRACE monthly solutions. For a detailed evaluation of the different filtering techniques we compared them on global and regional scale with different hydrological models (e.g. WGHM). Evaluation criteria for such comparisons are: wRMS, RMS-variability, annual/semi-annual signals and trends. We investigated as well which filter is most effective in terms of regional problems, since the characteristics of a filter are not the same throughout the whole Earth's grid and a global wRMS would not represent the features of each location.

A regional calculation requires the development of anti-leakage basin masks, depending on the chosen filter and on the particular basin. In fact, a side effect of filtering gravity fields as well as of limitations in spatial resolution, is the loss of signal intensity and hence a reduction of the signal amplitude (leakage effect). The stronger the smoothing the more amplitude is lost. Therefore, a

leakage reduction is needed. To maintain the amplitude and minimize the signal loss, time-constant scale factors (Landerer and Swenson 2012) are introduced. They are estimated using geophysical models (e.g. for continental hydrology: WGHM). Along the coastline scale factors are especially large since the low signal of the surrounding ocean is leaking into the coastal signal. The benefit of calculating time-dependent scale factors has also been investigated. A related paper describing all these issues is planned for end of 2016.

As for continental hydrology (Level-3.1), we will further improve and investigate appropriate leakage correction for the ocean and for Greenland and Antarctica (needed for Level-3.2). This is work under progress and shall be finished till June 2017.

5.3 Low degrees: degree 1 and C20

Level-3 generation requires the development and implementation of degree-1 (geocenter motion) variations, since they cannot be directly inferred from the GRACE and GRACE-FO observations. This information cannot be omitted without impacting the recovered mass variability, and is therefore needed when comparing, for example, GRACE with GNSS (Global Navigation Satellite System) or OBP (Ocean Bottom Pressure). The degree-1 variability is provided from regularly updated external data, such as SLR (Cheng et al. 2011), joint inversion of GPS, OBP and GRACE (Rietbroeck et al. 2012), or using global eustatic sea-level variations for the approximation of geocenter motion from GRACE (Bergmann et al. 2014). The latter will be used for Level-3.1, for Level-3.2 is still TBD.

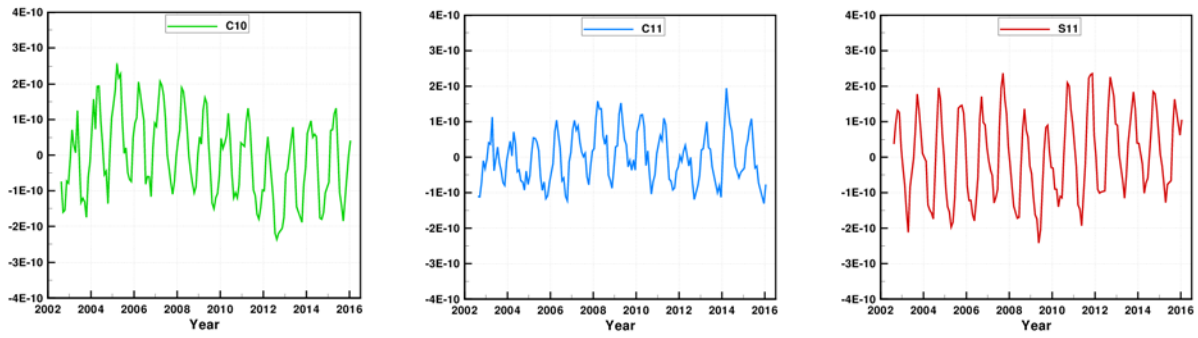

Fig. 5.1: degree-1 time series derived from GFZ RL05a using the method of Bergmann et al. 2014

Additionally to degree-1, the GRACE observed variations in coefficient C_{20} (Earth oblateness) are noisy and need to be replaced, for example by SLR derived values which are regularly provided by the Center for Space Research at the University of Texas (GRACE TN07, ftp://podaac.jpl.nasa.gov/allData/grace/docs/TN-07_C20_SLR.txt). The latter will be used for Level-3.1, for Level-3.2 is still TBD.

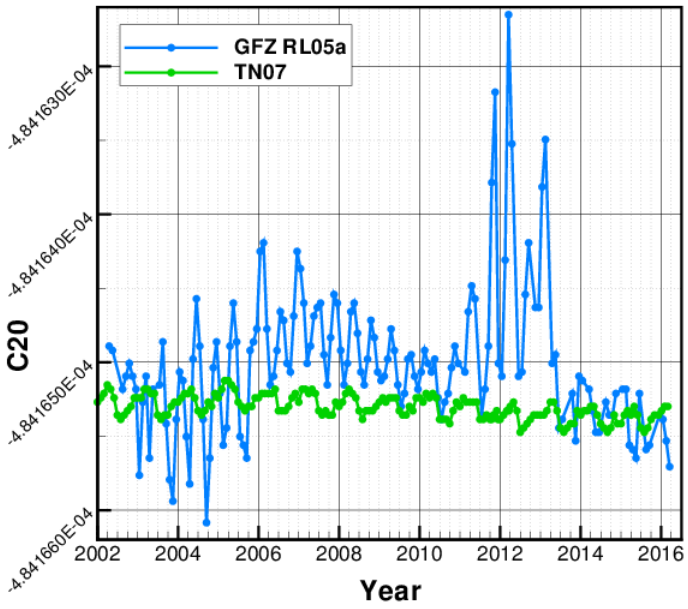

Fig. 5.2: C_{20} time series derived from GRACE (GFZ RL05a) and SLR (TN07).

5.4 Glacial Isostatic Adjustment (GIA)

A-posteriori correction of unmodeled signals such as glacial isostatic adjustment in presently and formerly glaciated regions is needed as well. For Greenland A et al. 2013 is adequate; for the Antarctic region, as of today, Ivins et al. 2013 or Whitehouse et al. 2012 are recommended and therefore have been implemented.

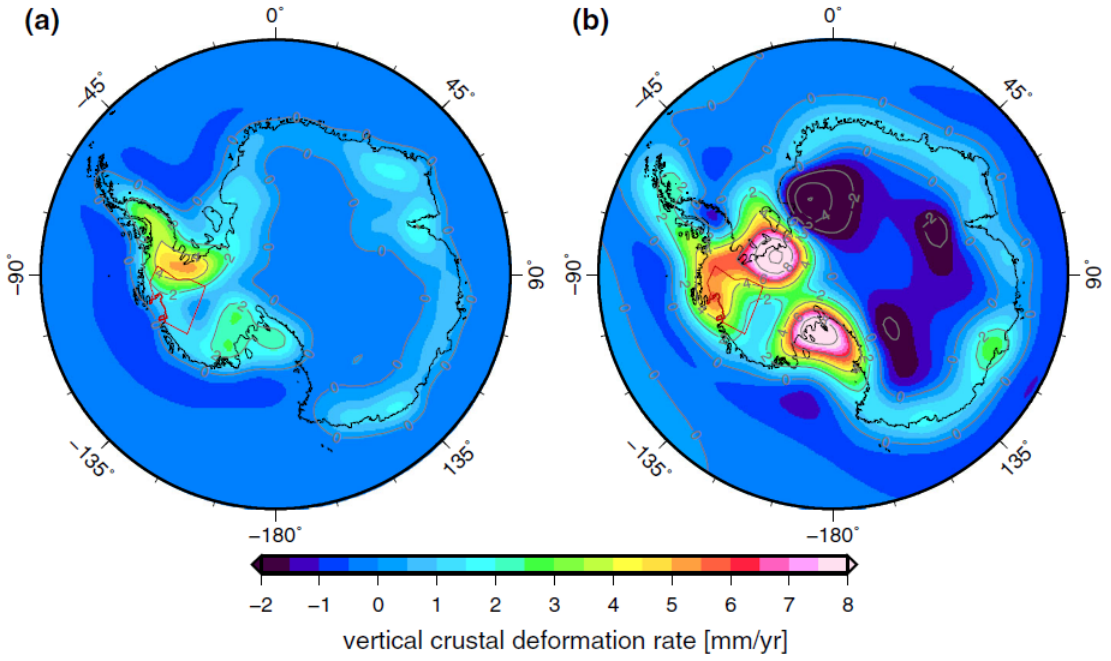

Fig. 5.3: Present-day GIA-induced vertical crustal deformation rates predicted by the models (a) IJ05_R2 (Ivins et al. 2013) and (b) W12a (Whitehouse et al. 2012). Figure taken from Groh et al. 2014.

5.5 Restore De-aliasing

GRACE non-tidal high-frequency atmospheric and oceanic mass variation models are routinely generated at GFZ as so-called Atmosphere and Ocean De-aliasing Level-1B (AOD1B) products to be added to the background static gravity model during GRACE monthly gravity field determination. AOD1B products are 6-hourly series of spherical harmonic coefficients up to degree and order 100 which are routinely provided to the GRACE Science Data System and the user community with only a few days time delay. These products reflect spatio-temporal mass variations in the atmosphere and oceans deduced from an operational atmospheric model and corresponding ocean dynamics provided by an ocean model. The variability is derived by subtraction of a long-term mean of vertical integrated atmospheric mass distributions and a corresponding mean of ocean bottom pressure as simulated with the ocean model.

In order to compare GRACE mass transport with e.g. OBP data this background model information has to be re-added over the oceans. For this, each analysis center provides also a GAC Level-2 product which is the mean of all applied AOD1B products over the corresponding month.

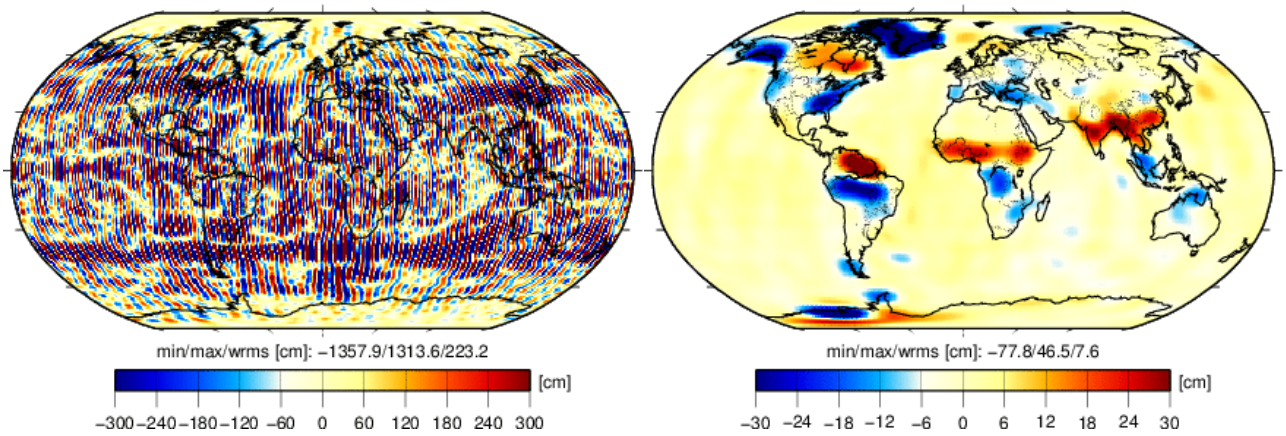

Fig. 5.4: GFZ RL05a GRACE Level-2 product (Sep 2007) (left) and preliminary Level-3.1 product (right) based on DDK2 filtering and C_{20} (TN07) substitution.

5.6 Summary: Planned Level-3 Product List

The following Level-3.1 and Level-3.2 products shall be generated and disseminated for each individual AC monthly solution and EGSIEM combined solution. The necessary corrections (Degree-1 coefficients, C_{20}, GIA, smoothing, leakage etc.) will be calculated according to models and methods as described above.

	Level-3.1	**Level-3.2**		
Application	Global	Land	Ocean	Ice
C20 substitution	yes	yes	yes	yes
Geocenter correction	yes	yes	yes	yes
GIA correction	yes	yes	yes	yes
Restore de-aliasing	yes (GAD)	no	yes (GAD)	no
Decorrelation & smoothing	DDK3	DDK3	DDK3	DDK3
Leakage correction	yes	yes	yes	yes
Synthesis to Grid	1°x1°	1°x1°	1°x1°	1°x1°

Note that the final models/procedures will be chosen at GFZ for Level-3.1 till October 2016 and for Level-3.2 till June 2017 (in the framework of the GRACE-FO project).

5.7 References

A, G., J. Wahr, and S. Zhong (2013): Computations of the viscoelastic response of a 3-D compressible Earth to surface loading: an application to Glacial Isostatic Adjustment in Antarctica and Canada. Geophysical Journal International, 192:557–572, doi:10.1093/gji/ggs030.

Bergmann-Wolf, I.,L. Zhang, and H. Dobslaw (2014): Global eustatic sea-level variations for the approximation of geocenter motion from GRACE. Journal of Geodetic Science, 4:37–48, doi:10.2478/jogs-2014-0006.

Cheng M., and J. Ries (permanently updated): Monthly estimates of C20 from 5 SLR satellites based on GRACE RL05 models. GRACE TN07, Center for Space Research, The University of Texas at Austin

Cheng, M., J.C. Ries, and B.D. Tapley (2011): Variations of the Earth's figure axis from satellite laser ranging and GRACE. Journal of Geophysical Research (Solid Earth), 116(B15):1409–+, doi:10.1029/2010JB000850.

Groh, A., H. Ewert, R. Rosenau, E. Fagiolini, C. Gruber, D. Floricioiu, W. Abdel Jaber, S. Linow, F. Flechtner, M. Eineder, W. Dierking, and R. Dietrich (2014); Mass, Volume and Velocity of the Antarctic Ice Sheet: Present-Day Changes and Error Effects. Surveys in Geophysics, 35:1481–1505, doi:10.1007/s10712-014-9286-y.

Ivins, E. R., T.S. James, J. Wahr, E.J.O. Schrama, F.W. Landerer, and K.M. Simon (2013): Antarctic contribution to sea level rise observed by GRACE with improved GIA correction. Journal of Geophysical Research (Solid Earth), 118:3126–3141, doi:10.1002/jgrb.50208.

Kusche, J. (2007): Approximate decorrelation and non-isotropic smoothing of time-variable GRACE-type gravity field models. Journal of Geodesy, 81:733–749, doi:10.1007/s00190-007-0143-3.

Landerer, F. W., and S.C. Swenson (2012): Accuracy of scaled GRACE terrestrial water storage estimates. Water Resources Research, 48:4531, doi:10.1029/2011WR011453.

Rietbroek, R., M. Fritsche, S.-E. Brunnabend, I. Daras, J. Kusche, J. Schröter, F. Flechtner, and R. Dietrich (2012): Global surface mass from a new combination of GRACE, modelled OBP and reprocessed GPS data. Journal of Geodynamics, 59:64–71, doi:10.1016/j.jog.2011.02.003.

Swenson, S. and J. Wahr (2006): Post-processing removal of correlated errors in GRACE data. Geophysical Research Letters, 33:8402–+, doi:10.1029/2005GL025285.

Whitehouse, P., M. Bentley, G. Milne, M. King, and I. Thomas (2012): A new glacial isostatic adjustment model for Antarctica: calibrated and tested using observations of relative sea-level change and present-day uplift rates. Geophys J Int 190(3):1464–1482. doi:10.1111/j.1365-246X.2012.05557.x

6.Output and Dissemination

Output: The basic results of the combination service are the monthly combinations of gravity fields, either on solution level, or on normal equation level. The original parameters of the combination are the spherical harmonic coefficients and their formal errors (L2-products) in the ICGEM-format. They are transformed to user-friendly global grids of equivalent water height (L3-products). Further internal products are the combined NEQs in SINEX format, that are provided via FTP-server for all associated EGSIEM members.

Dissemination (EGSIEM internally): Via ftp (ubern@dl.aiub.unibe.ch) or by http-access (http://dl.aiub.unibe.ch/data/egsiem/private/) all EGSIEM WP2 and WP4 internal data and also the freely available products are accessible. Access is restricted to the EGSIEM ACs and is protected by password.

The following sub-directories were established:

GRAVITY:	L2- and L3-products sorted by AC
LEO-Orbits:	Kinematic orbits sorted by AC, satellite and year
NEQ:	Normal equations sorted by AC, satellite, observation type (GPS: GPS-only, KBR: K-band + GPS, Model_corr: monthly mean of background models) and year
org:	Space for the ACs to store additional information, sorted by AC
Repro-15:	Reference frame products provided by AIUB, sorted by year and type (CLK: clock corrections, ORB: GPS orbits, STA: station information).

Dissemination (users): The L2-products of the individual ACs and their combinations will be disseminated via the International Center for Global Earth Models (ICGEM, http://icgem.gfz-potsdam.de/ICGEM/) and via the currently developed ISDC2.0, both at GFZ. The L3-products will be visualized and distributed via the EGSIEM plotter (http://plot.egsiem.eu/).

7.Glossary

AC	Associated processing Center
AOD1B	Atmosphere and Ocean De-aliasing Level-1B
EWH	Equivalent Water Height
GIA	Global Isostatic Adjustment
GNSS	Global Navigation Satellite System
GPS	Global Positioning System
ICGEM	International Center for Global Earth Models
IERS	International Earth Rotation Service
IGS	International GNSS Service
ISDC	Information System and Data Center
IUGG	International Union of Geodesy and Geophysics
MAD	Median Absolute Deviation
MEWH	Mean Equivalent Water Height
NEQ	Normal Equation
OBP	Ocean Bottom Pressure
SDS	Science Data System
SH	Spherical Harmonic
SINEX	Solution INdependent Exchange format
SLR	Satellite Laser Ranging
VCE	Variance Component Estimation
WGHM	WaterGAP Global Hydrological Model
wRMS	weighted Root Mean Square
wSTD	weighted STandard Deviation